

2025 DRAGON 6 SYMPOSIUM

14-18 JULY 2025

[PROJECT ID. 95462]

INVERTING MOUNTAIN METEOROLOGY FROM CRYOSPHERIC REMOTE SENSING AND ECOHYDROLOGICAL MODELLING (IMMERSE)





2025 Dragon 6 Symposium

THURSDAY, 17/JULY/2025: 11:00 - 12:30

ID. 95462

PROJECT TITLE: INVERTING MOUNTAIN METEOROLOGY FROM CRYOSPHERIC REMOTE SENSING AND ECOHYDROLOGICAL MODELLING (IMMERSE)

PRINCIPAL INVESTIGATORS: FRANCESCA PELLICCIOTTI AND MASSIMO MENENTI

CO-AUTHORS: EVAN MILES, KUN YANG, LI JIA, YUBAO QIU, CHAOLEI ZHENG, SHAOTING REN, ACHILLE JOUBERTON, HARUKI HAGIWARA, JIU CHEN, MENGYUAN CUI, WANGKAN SHE

PRESENTED BY: MASSIMO MENENTI CAS INSTITUTE FOR TIBETAN PLATEAU RESEARCH (ITP)

Outline



Project overview

Approach

Highlihts and First Results

Reporting

YS short presentations

Objectives and Expected Results

Goal: a novel, holistic understanding of the changing cryosphere and hydrosphere of HMA through model developments and an increasing amount of high resolution satellite observations.

Approach: Modelling blue, green and white water fluxes using very diverse spaceborne observations

Deliverables:

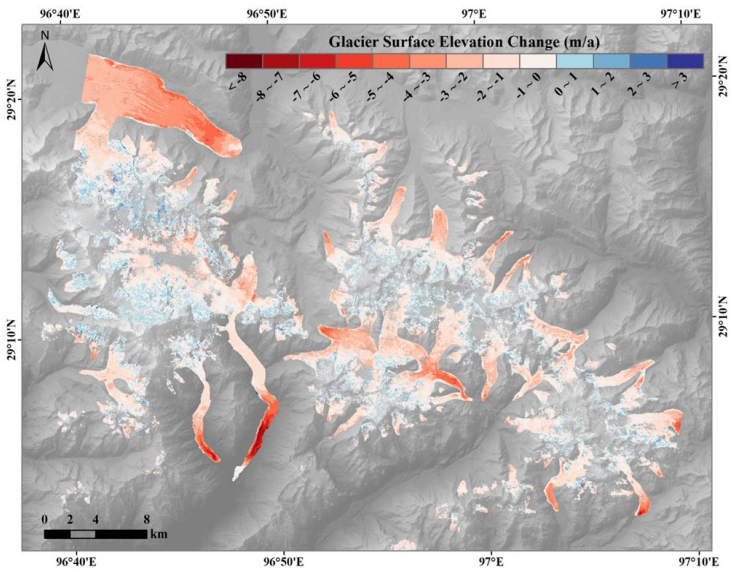
i. high-resolution land surface patterns and changes across HMA in key catchments;
ii. demonstration and first applications of a method to invert meteorological biases from Earth Observation data;
iii. catchment scale estimates of glacier melt, mass balance and snow cover, and their spatial and temporal variability;
iv. hyper resolution simulations of blue and green water fluxes at the 10 study sites for historic and future periods;

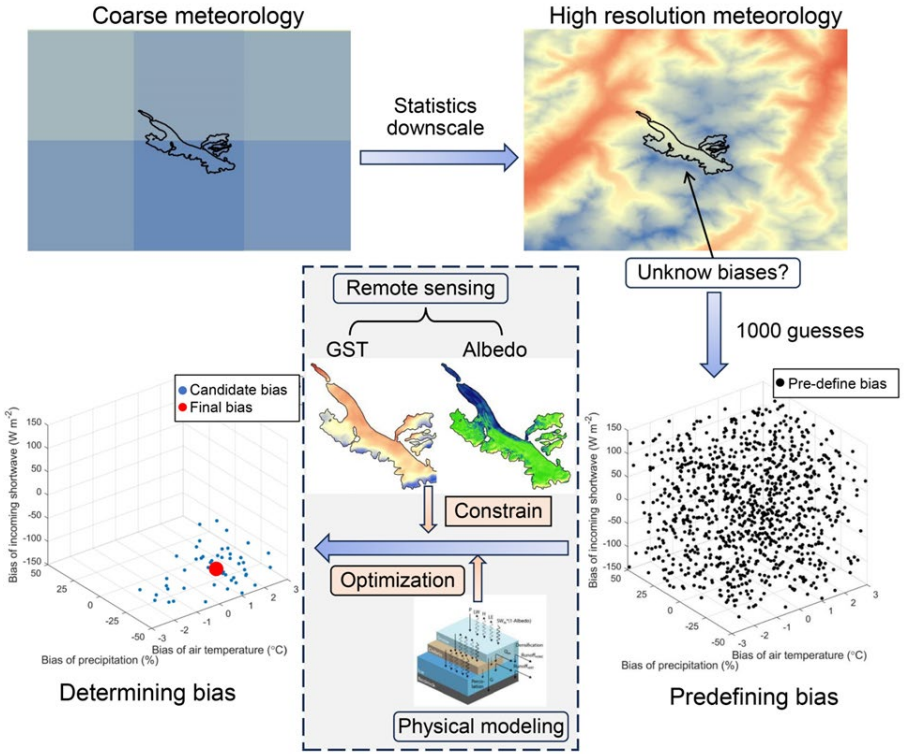
IMMERSE (ID. 95462) Project Overview

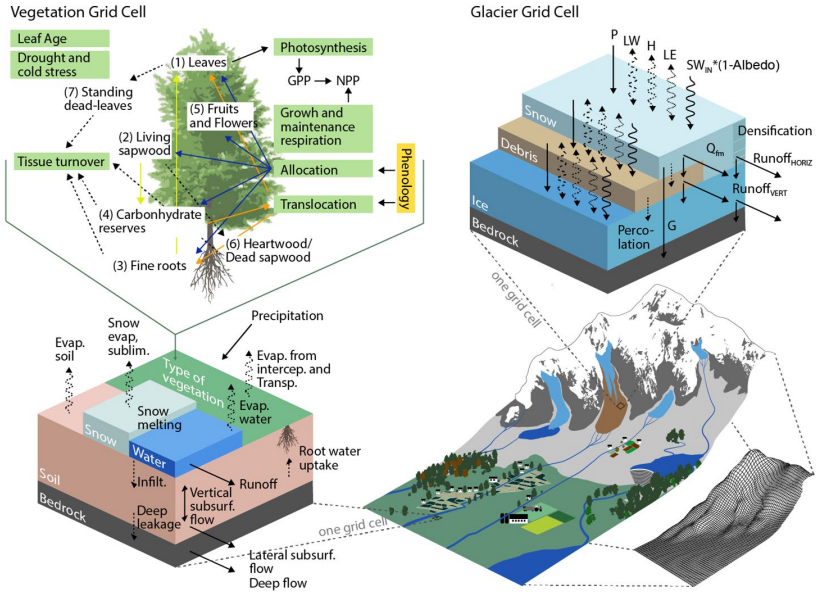
WP1: Satellite observations of water tower processes

WP2: Inversion of climate reanalysis biases from WP1 data and physical modelling

WP3: Hyper-resolution ecohydrological modelling







IMMERSE (ID. 95462) Study Sites

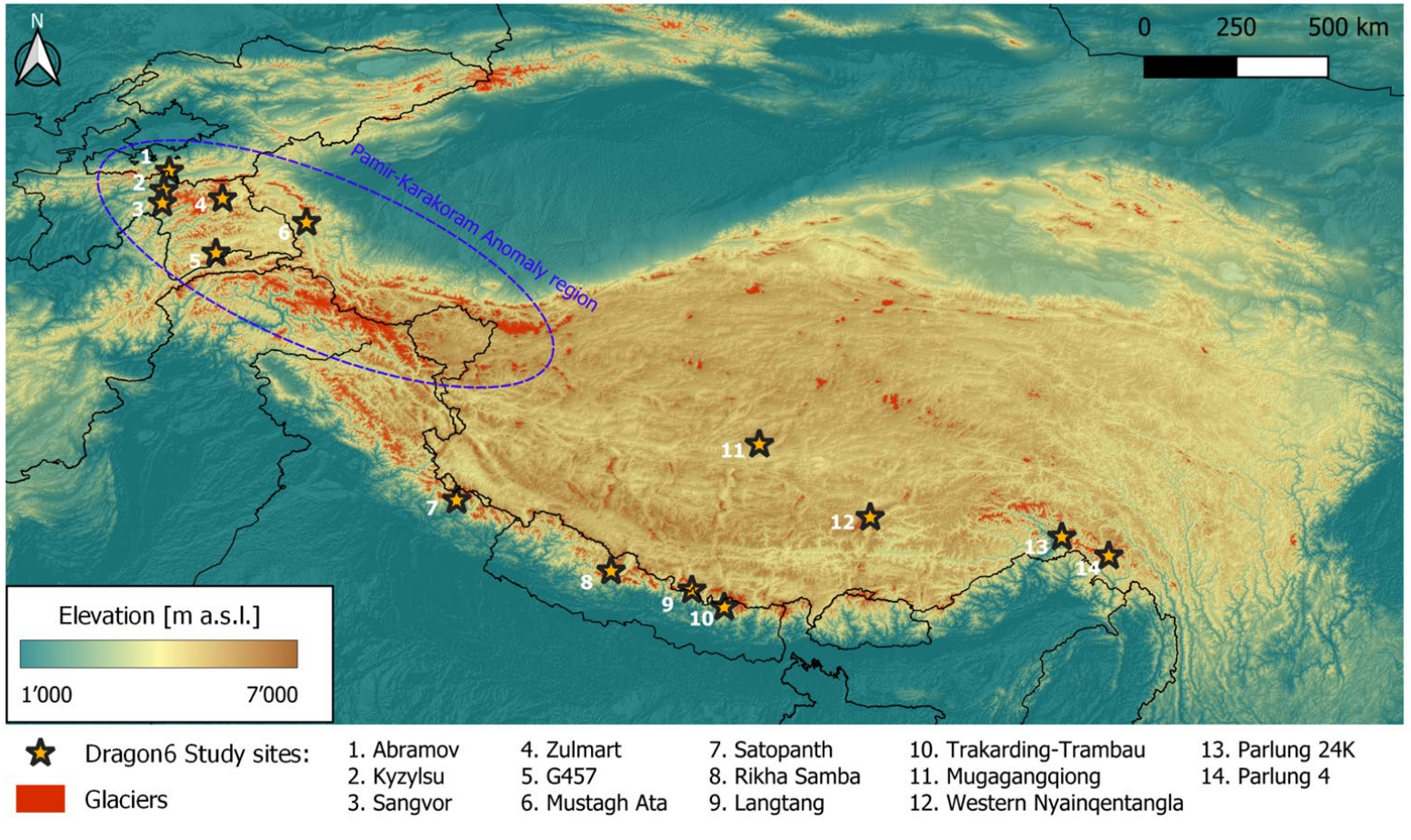
New focus on Pamir region:

- complex processes, moderate uncertainty

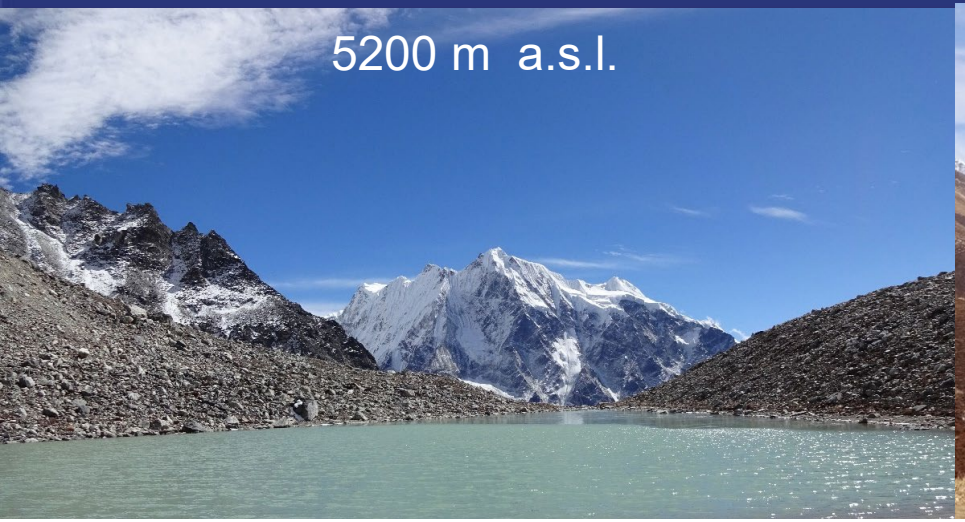
- extend new baseline data (PAMIR project)

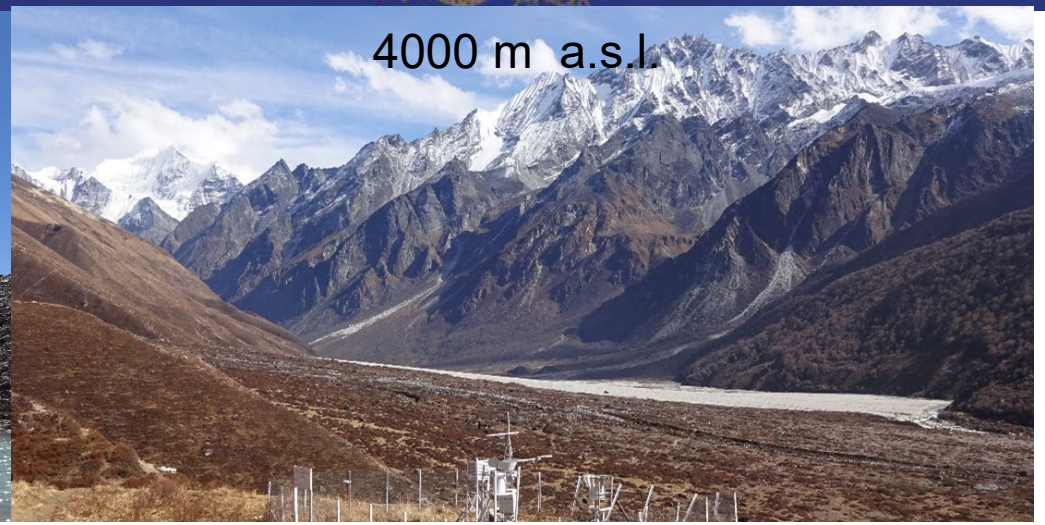
- create evidence base for Pamir-Karakoram Anomaly

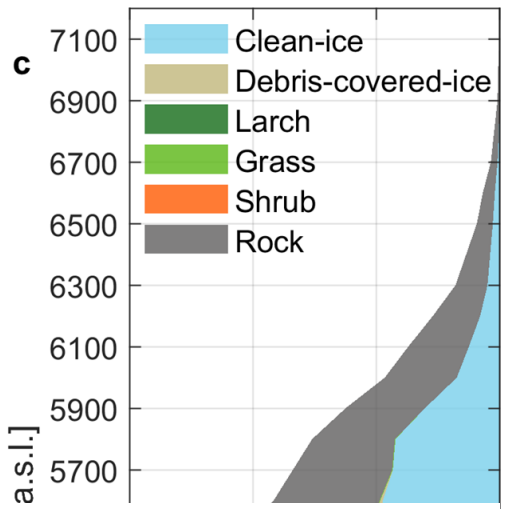
- nearly all sites planned previously visited by project team



Motivation: glacierized catchment



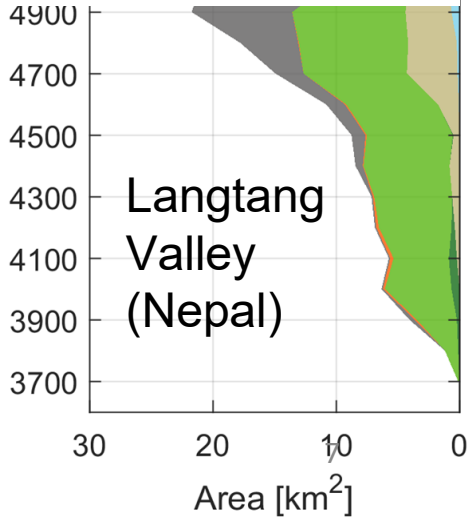




Understanding blue, green and white fluxes requires discriminating water phases in water inflow, outflow and stocks



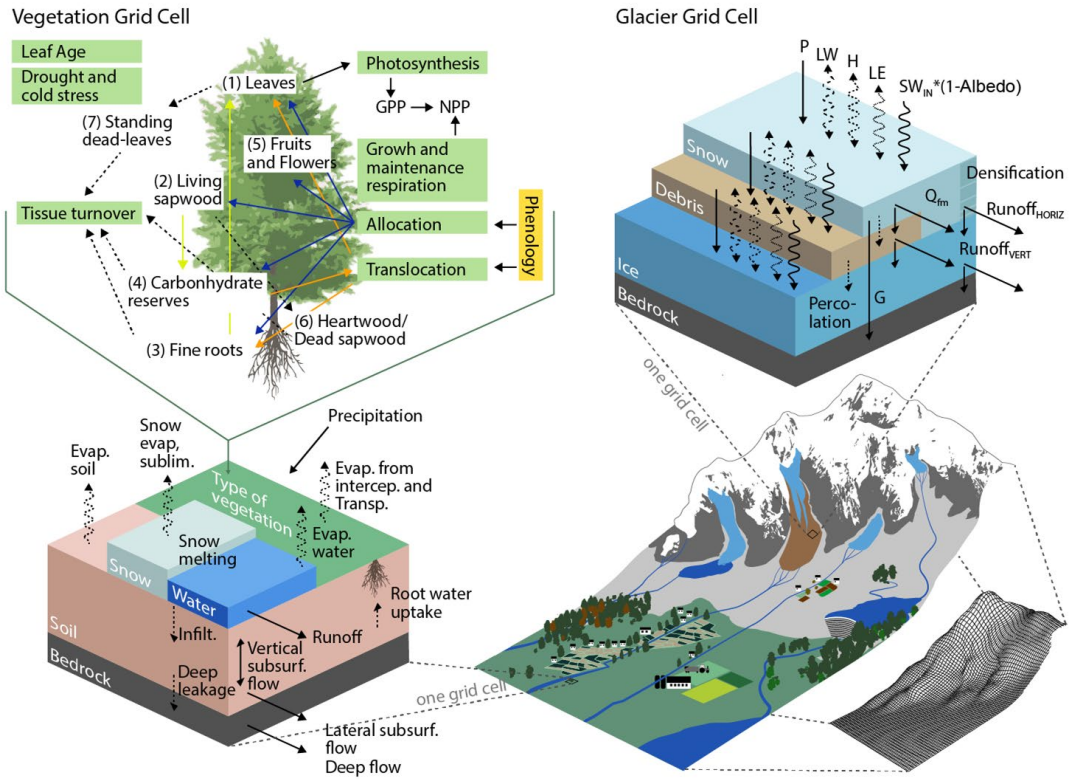




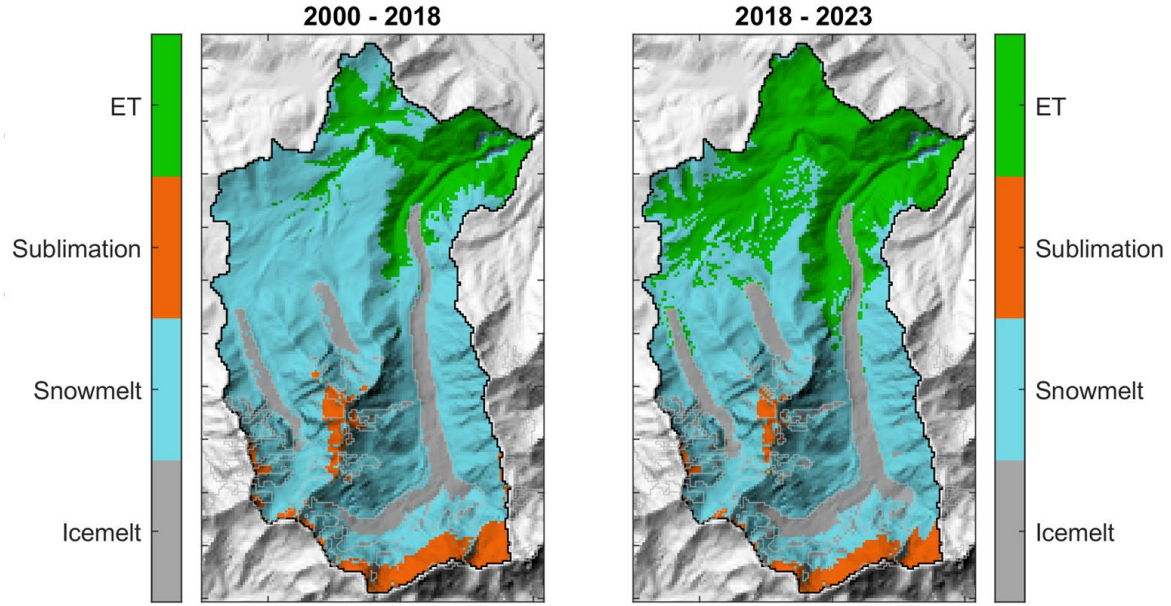
Ecohydrological modelling

Hyper-resolution modelling

Tethys-Chloris model forced with bias-corrected reanalysis data (ERA5-Land)



Jouberton et al. In review

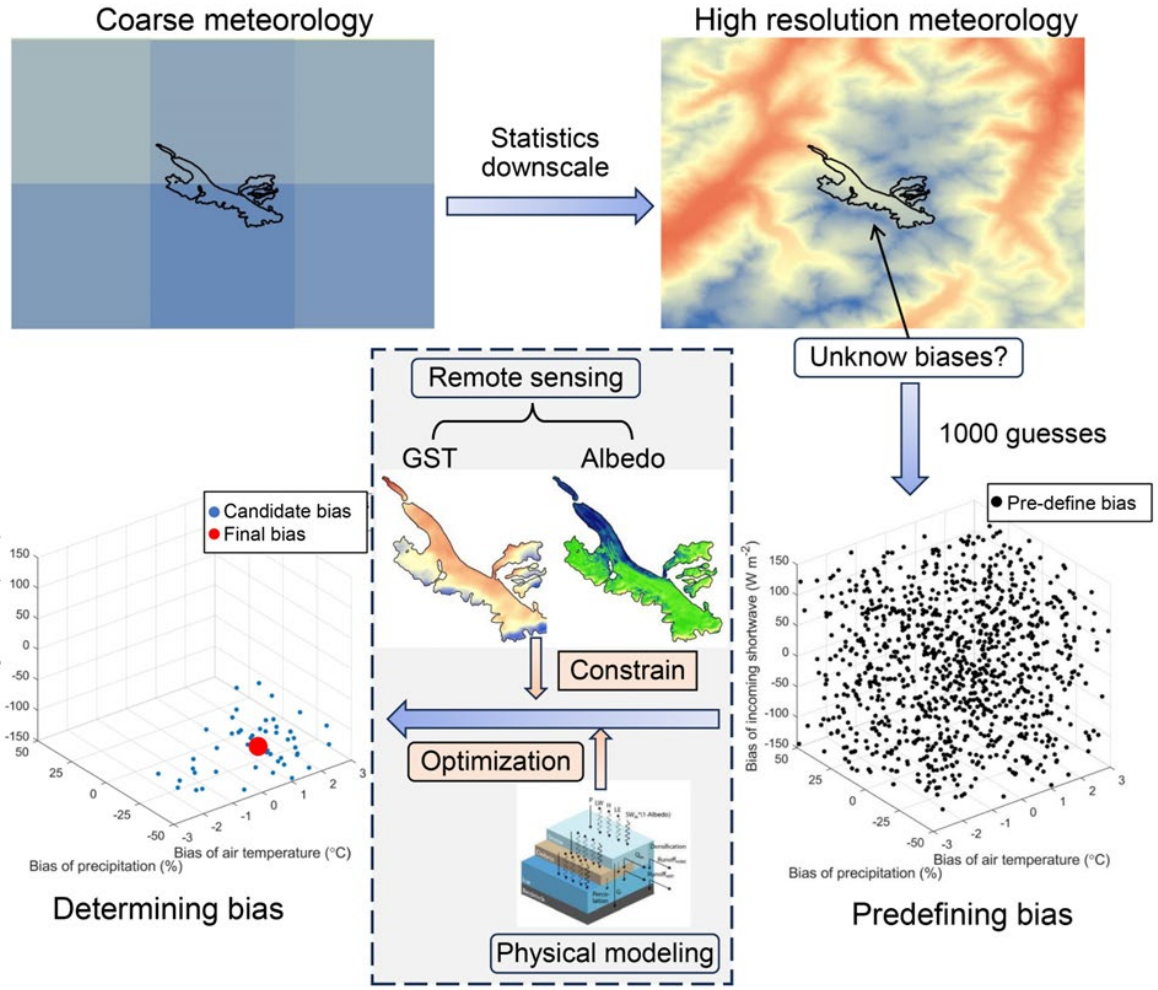


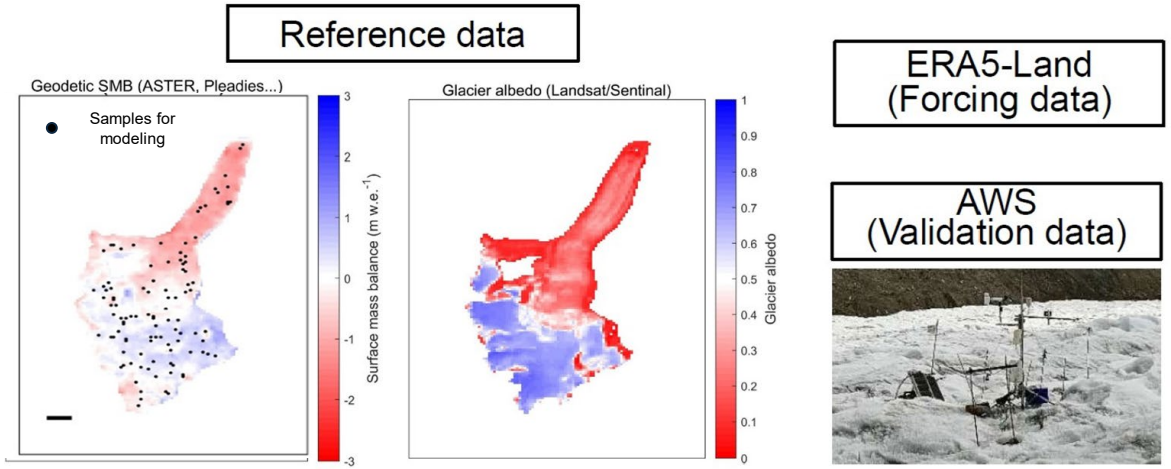
Example of land-surface model results in western HMA

- Evapotranspiration becomes the dominant water phase change process in more areas in recent years
- Sublimation is the dominant ablation process at highest elevations

Reanalysis bias correction

Challenge: reanalysis data has unknown biases





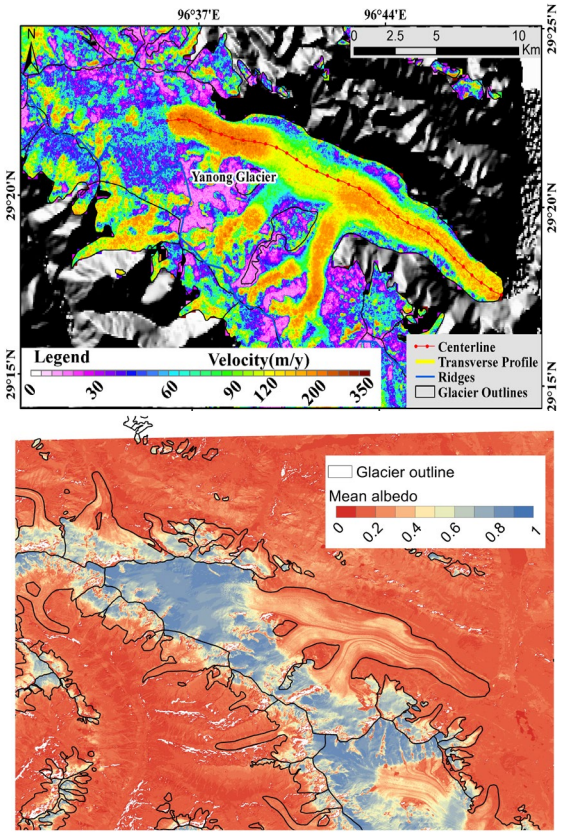
Can we infer these biases?

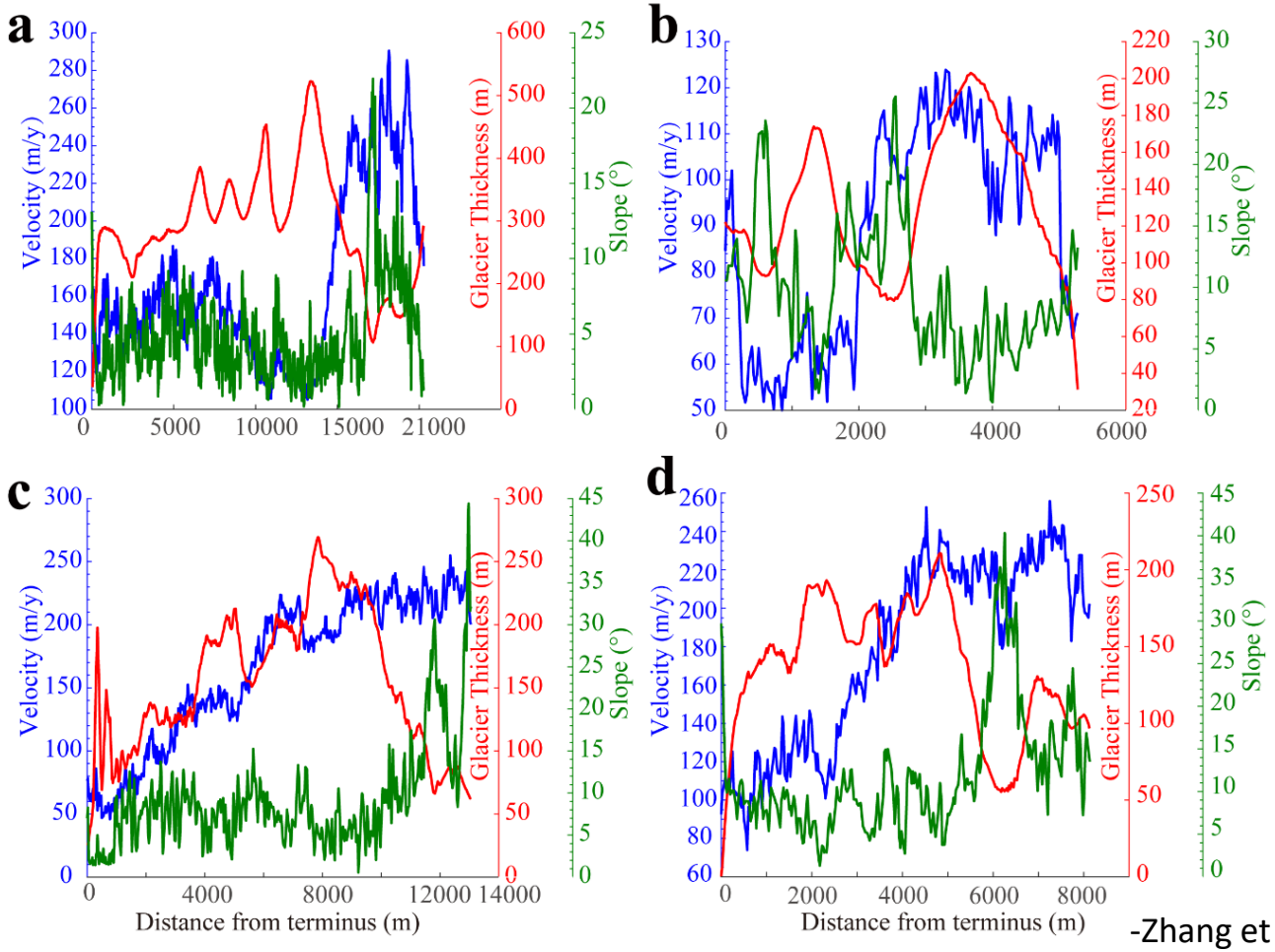
Concept:

1. Downscale
2. Monte Carlo model simulations
3. Optimize bias against ***satellite albedo and mass balance***
4. Evaluate against local measurements

Glacier albedo and flow

- Updated maps of glacier surface velocity in the Parlung Zangbo Basin;
- Glacier motion mechanisms using central flowline and transversal velocity profiles of four typical glaciers





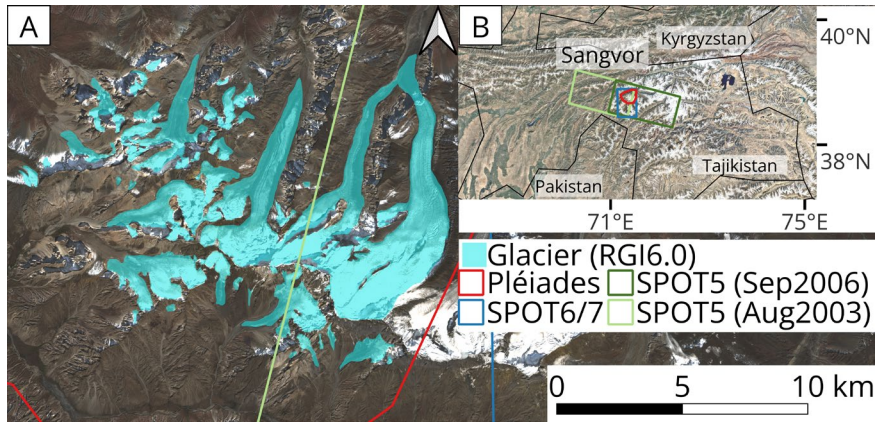
-Zhang et al., 2021

Annual mean centerline glacier velocity (blue line) versus glacier thickness (red line) versus slope (green line): (a) Yanong Glacier (b) Parlung No.4 Glacier (c) Azha and (d) Xueyougu Glacier

(Zhang et al. 2021)

Ice and snow volume changes

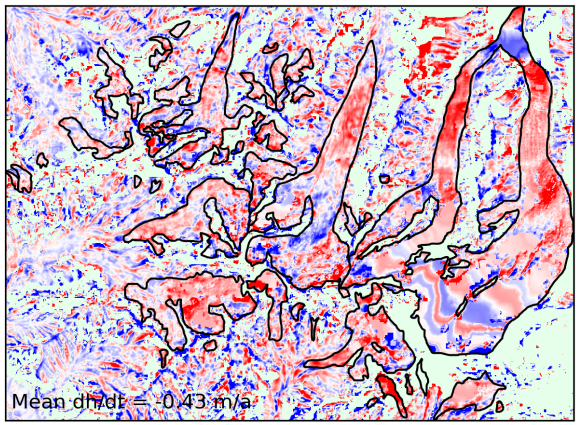
Insights from high-resolution DEM time series



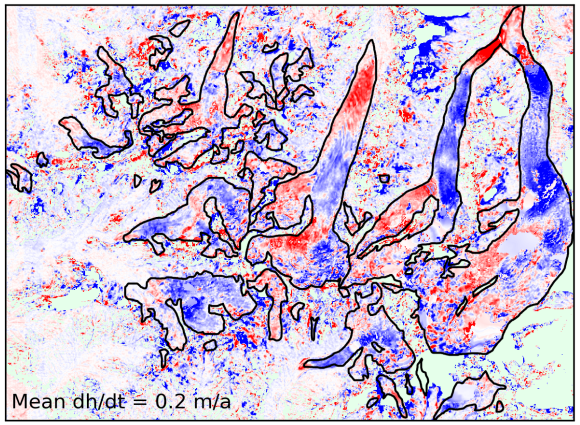
Study site: Sangvor, Tajikistan

1. Surge event between 2006 and 2014?
2. Huge elevation gain between 2014 and 2019?
3. Glaciers is decreasing rapidly since 2019?

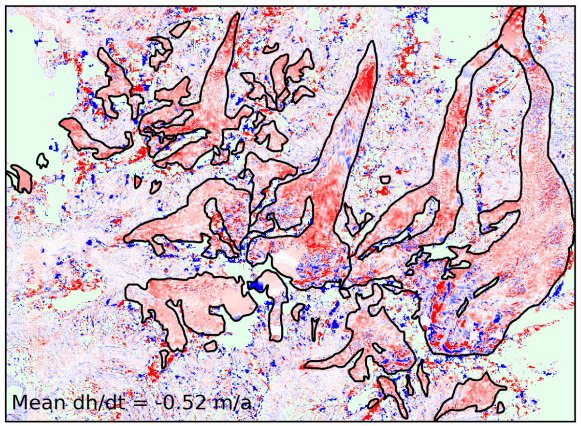
2006 2014 2019 2022 2024 Year



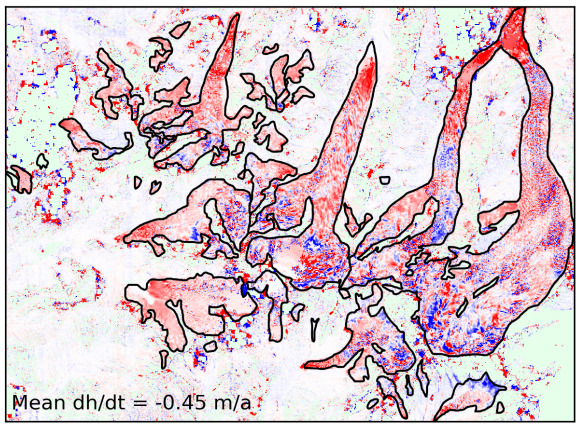
Mean dh/dt: -0.43 ± 0.15 [m/a]



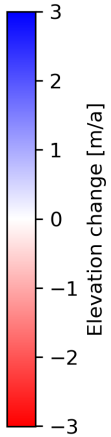
Mean dh/dt: +0.2 ± 0.10 [m/a]



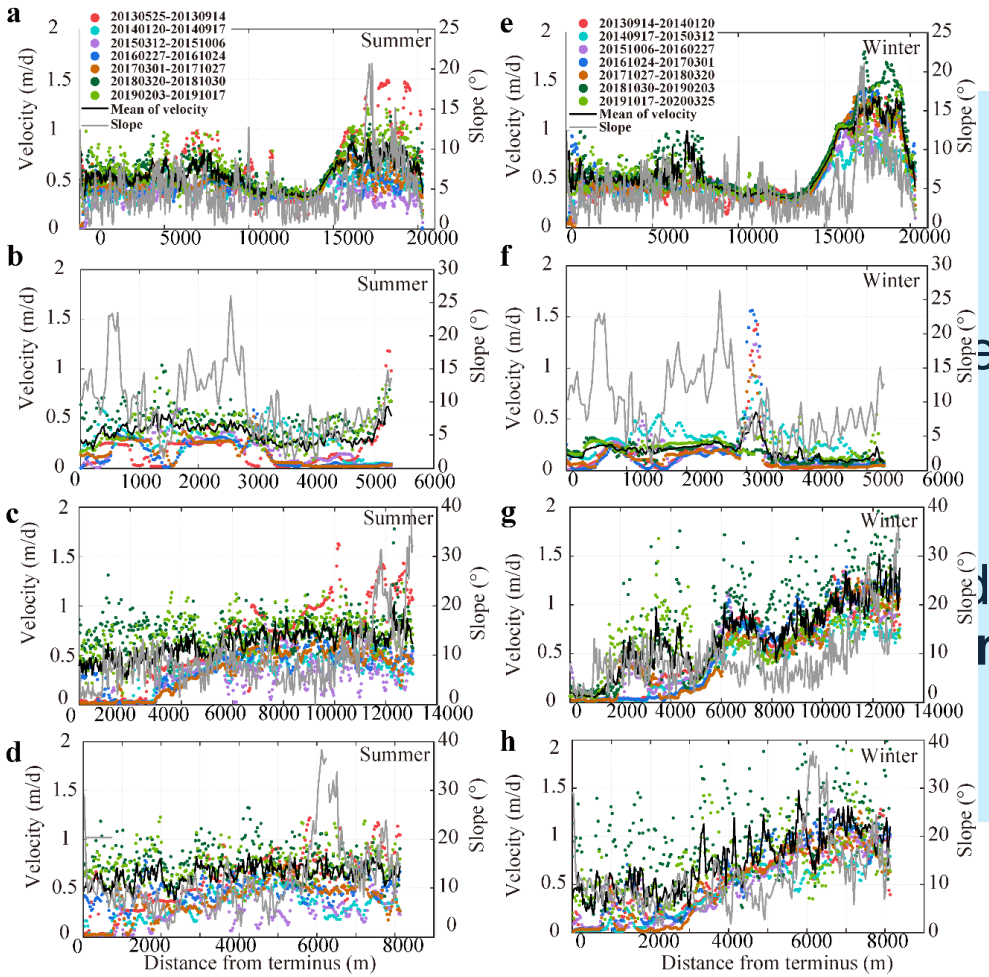
Mean dh/dt: -0.52 ± 0.18 [m/a]



Mean dh/dt: -0.45 ± 0.29 [m/a]

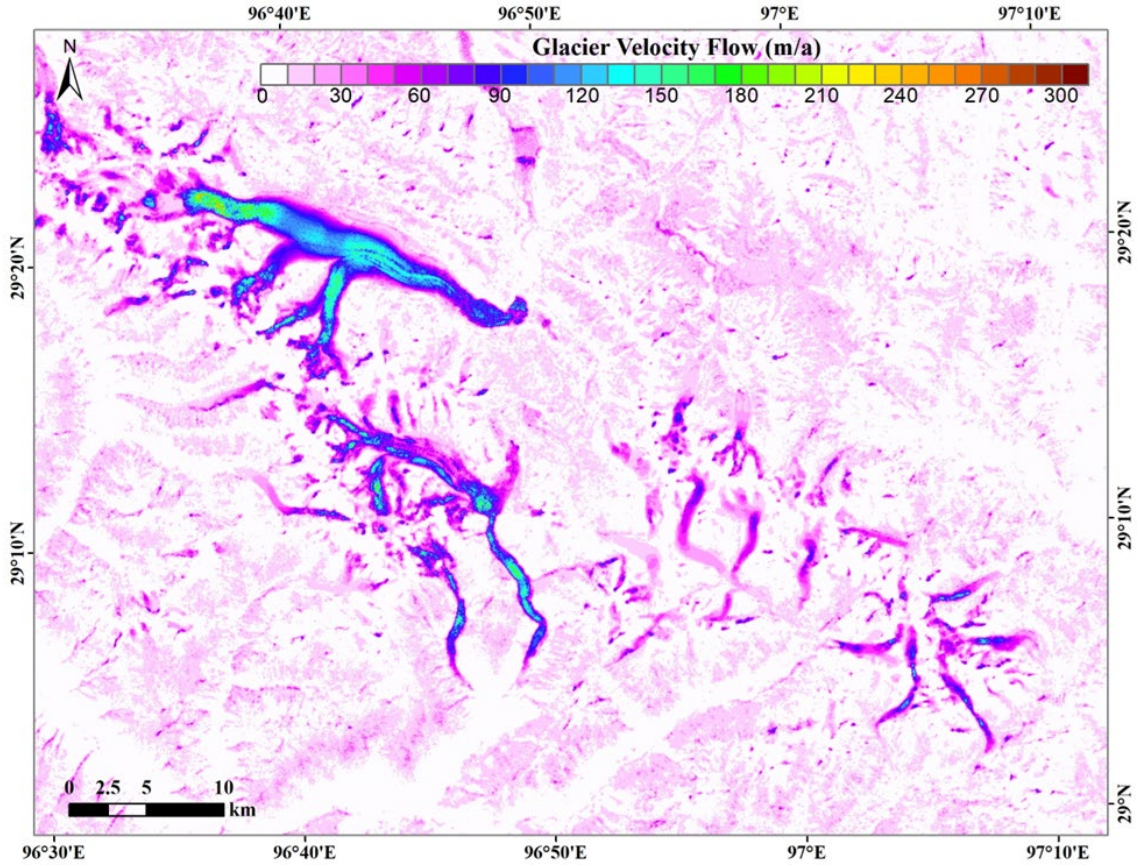


Variability of glacier velocity



eature

l from
nel-2;



-Zhang et al., 2021

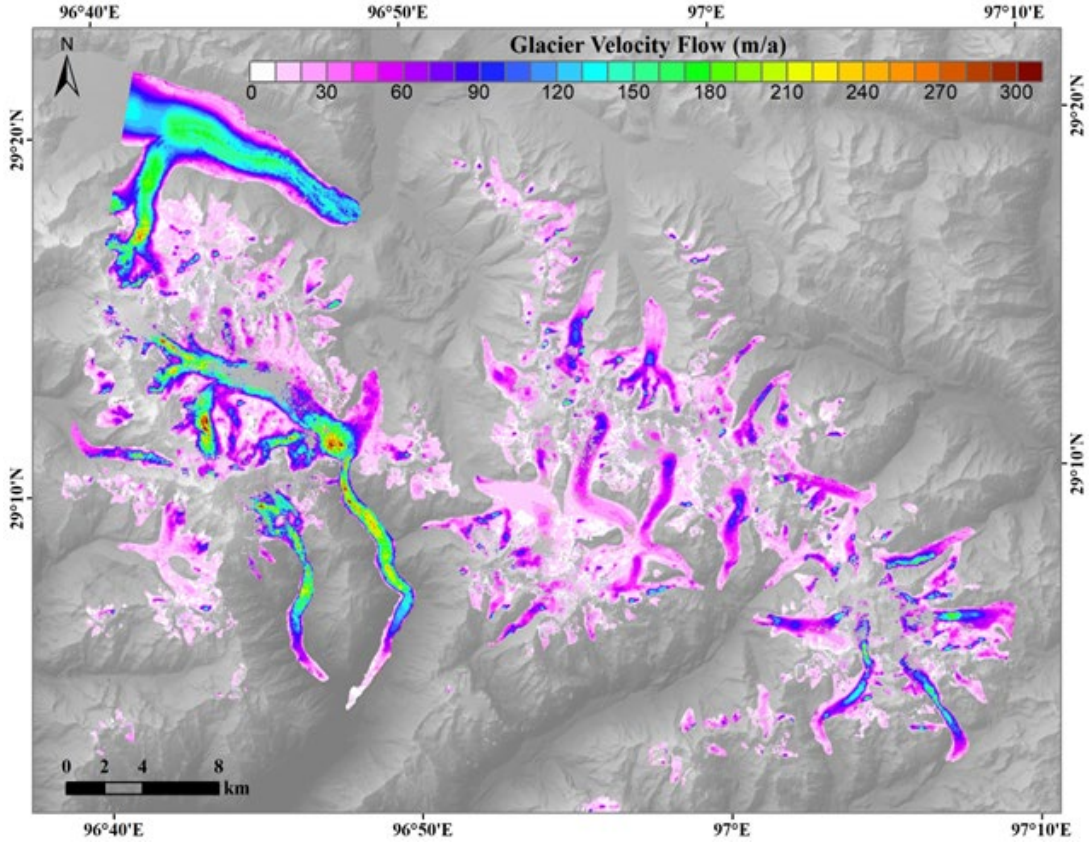
Summer (left, 2013–2019) and winter (right, 2013–2020) center flowline velocities versus vs. distance from terminus: Yanong Glacier (a and e) Parlung No.4 Glacier (b and f); Azha (c and g) and Xueyougu Glacier (d and h); mean velocity (black solid line)

Mean annual glacier velocity in the Parlung Zangbo Basin during 2013–2022

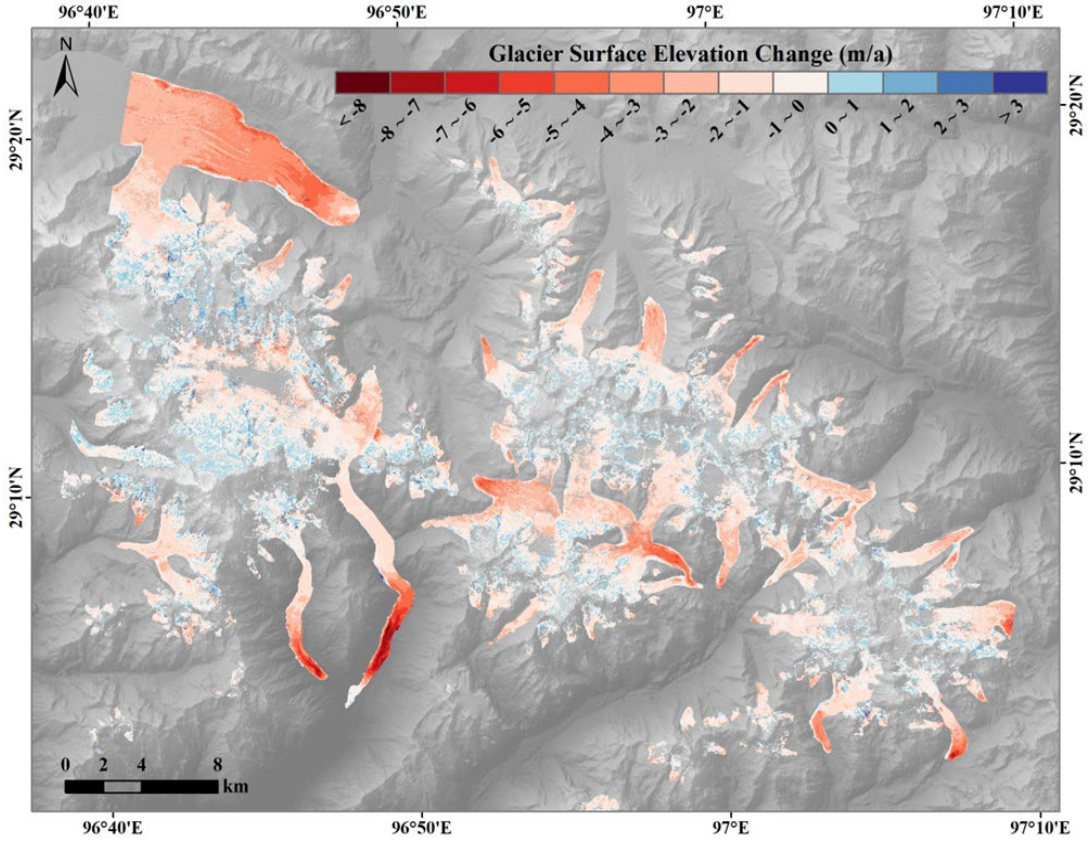
(Zhang et al. 2021)

Glacier surface velocity and volume changes

Combining RS datasets to yield reliable information at regional scales

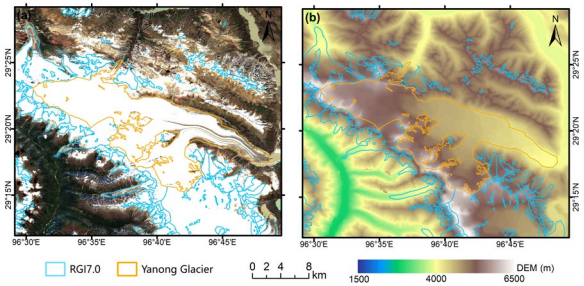


Mean annual glacier velocity in the Parlung Zangbo Basin during 2013–2022

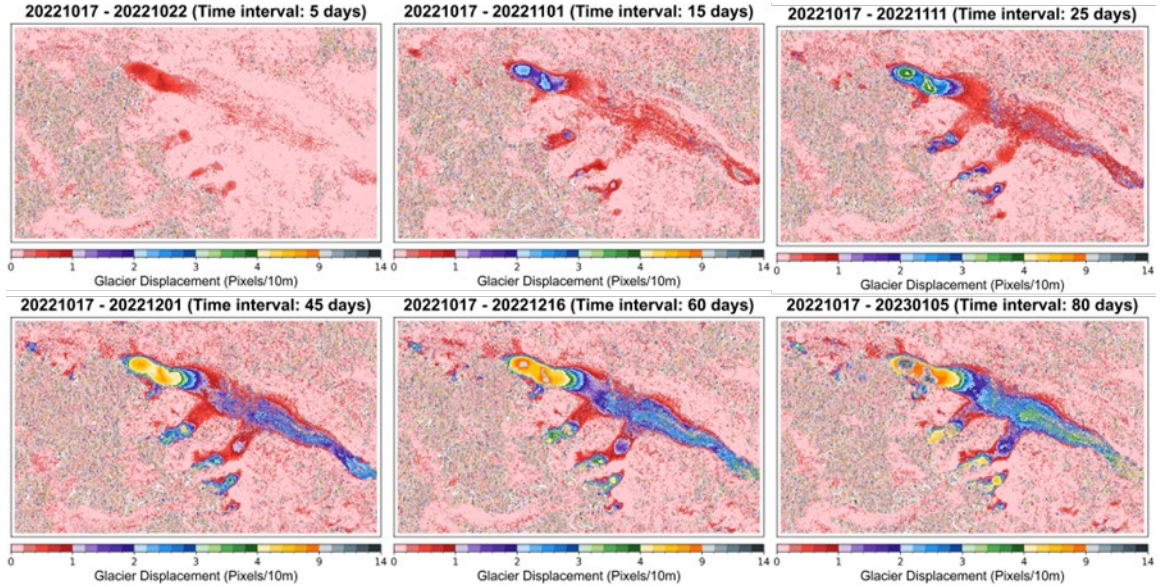


Annual thinning rate, same domain

Optimal time intervals for optical image cross-correlation

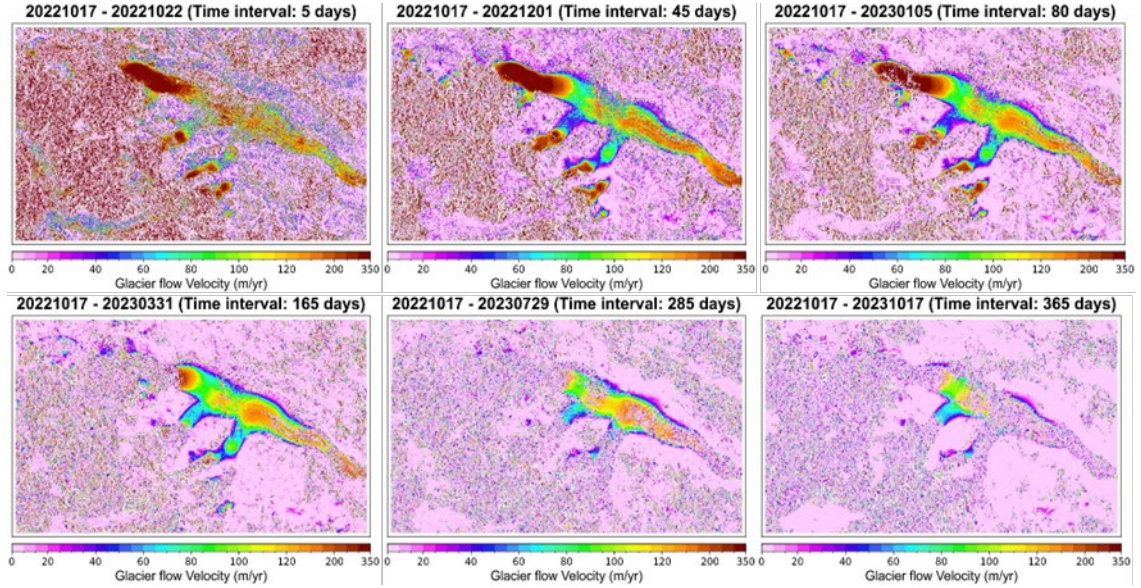


- **Study area**: Yanong Glacier in the southeastern Tibetan Plateau
- **Data**: Sentinel-2 MSI Products; **Method**: COSI-Corr
- The appropriate time interval: **45 and 120 days**
  - ✓ **Short time interval**: the displacement is too small to be detected
  - ✓ **Long time interval**: lose the correlation (the surface morphology of glaciers changes)



The glacier displacements

(Using image pairs with **different time intervals** and the **COSI-Corr** method)



The glacier flow velocities

(Using image pairs with **different time intervals** and the **COSI-Corr** method)

(Chen et.al., 2025 manuscript)

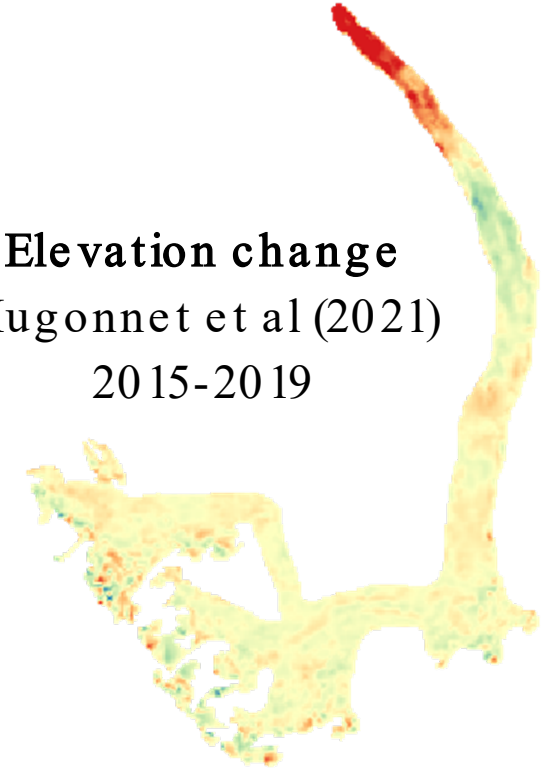
Glacier elevation changes vs. mass balance

Continuity equation _usable for local or regional datasets

$$\frac{dH}{dt} = SMB - \nabla * \boldsymbol{q}$$

Fortambek Glacier, Pamir

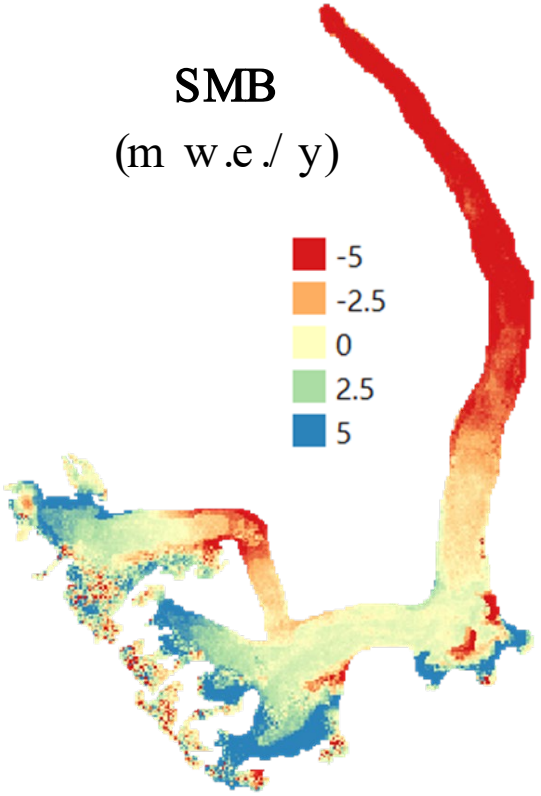




Elevation change
Hugonnet et al (2021)
2015-2019

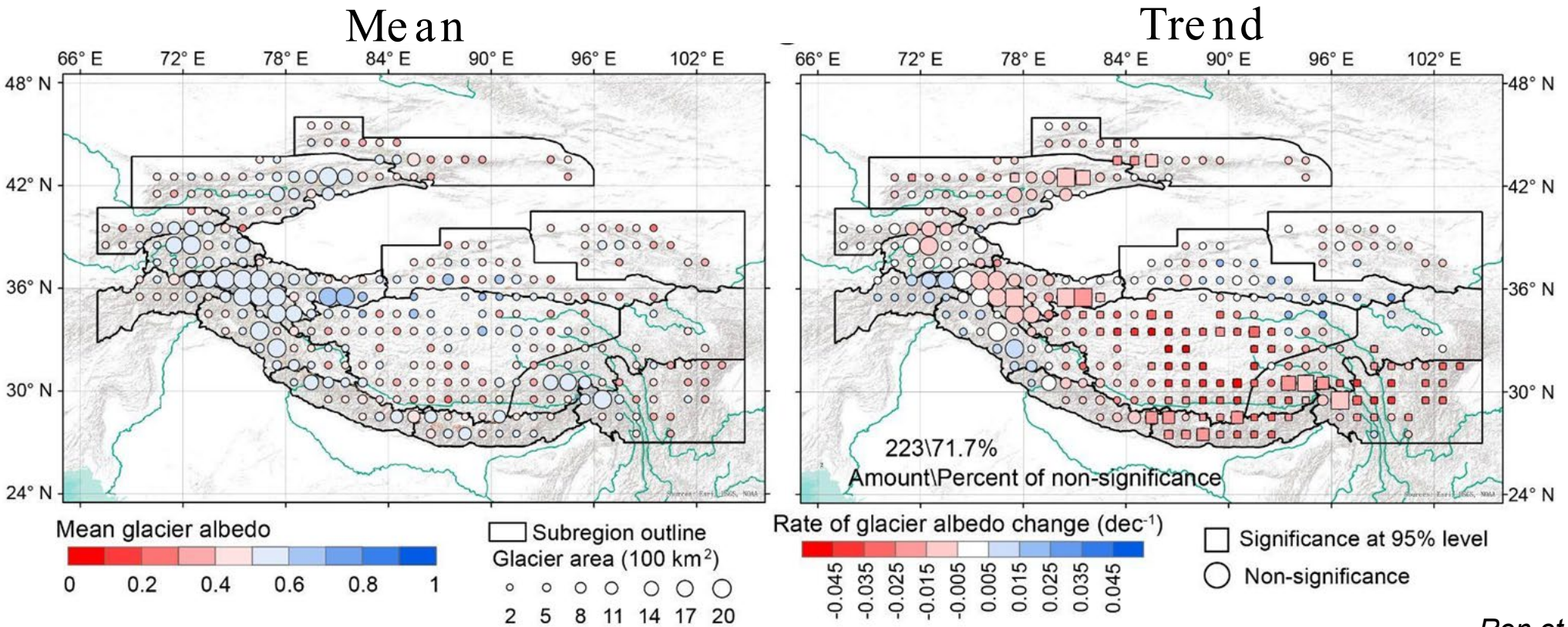


Surface velocity
Millan et al (2022)
2017-2018



Time series of glacier albedo

Surface albedo reveals heterogenous glacier changes annually, seasonally, altitudinally

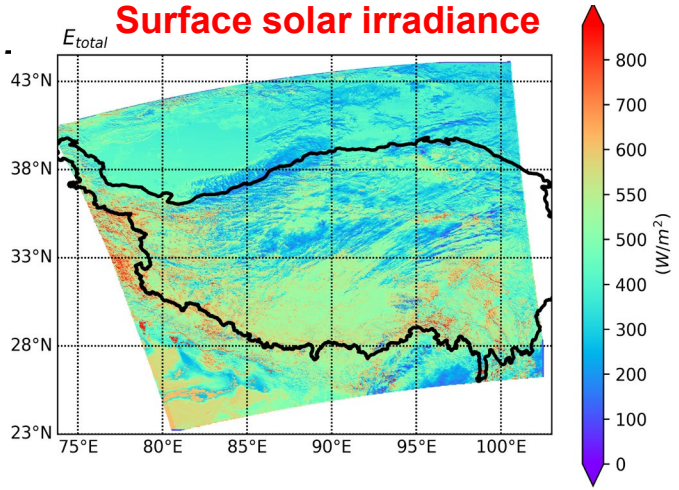


Ren et al. 2024

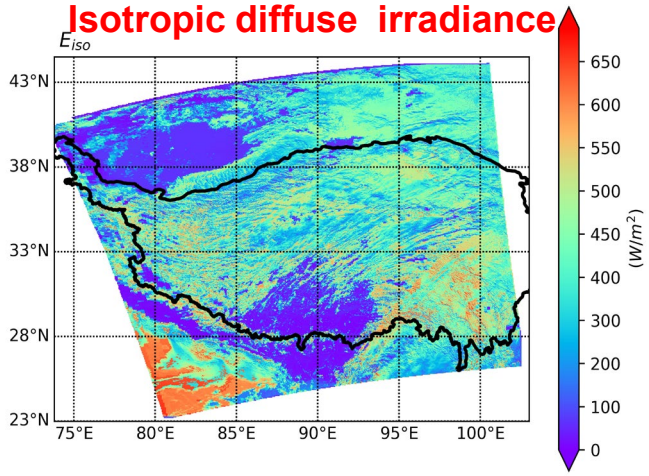
Glacier albedo in 2001-2020 in High Mountain Asia (**MODIS; Landsat-5/7/8/9, Sentinel-2**)

Retrieval of surface albedo

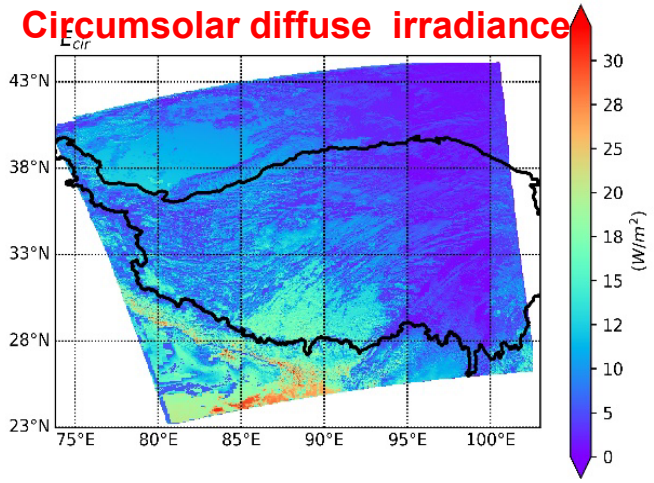
Surface solar irradiance



Isotropic diffuse irradiance

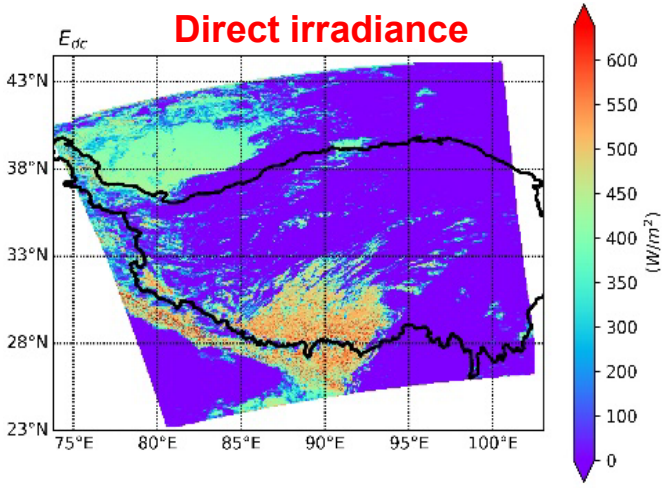


Circumsolar diffuse irradiance

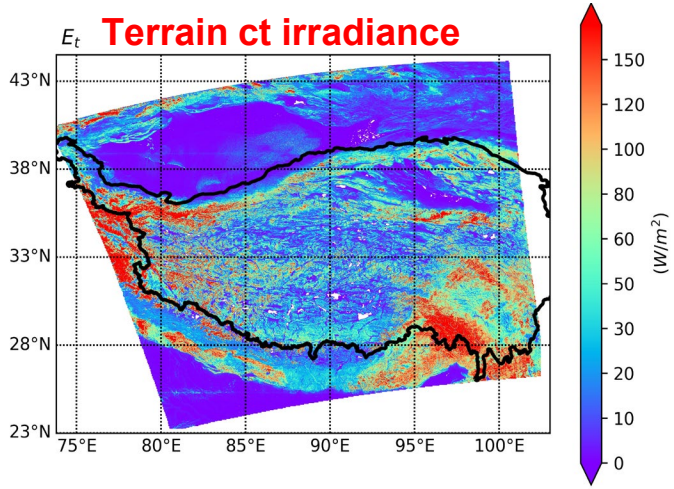


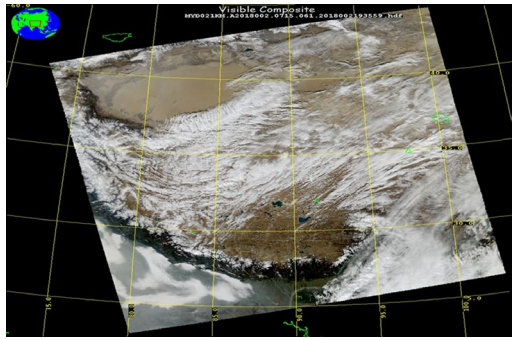
-Jia et al., 2024

Direct irradiance



Terrain ct irradiance



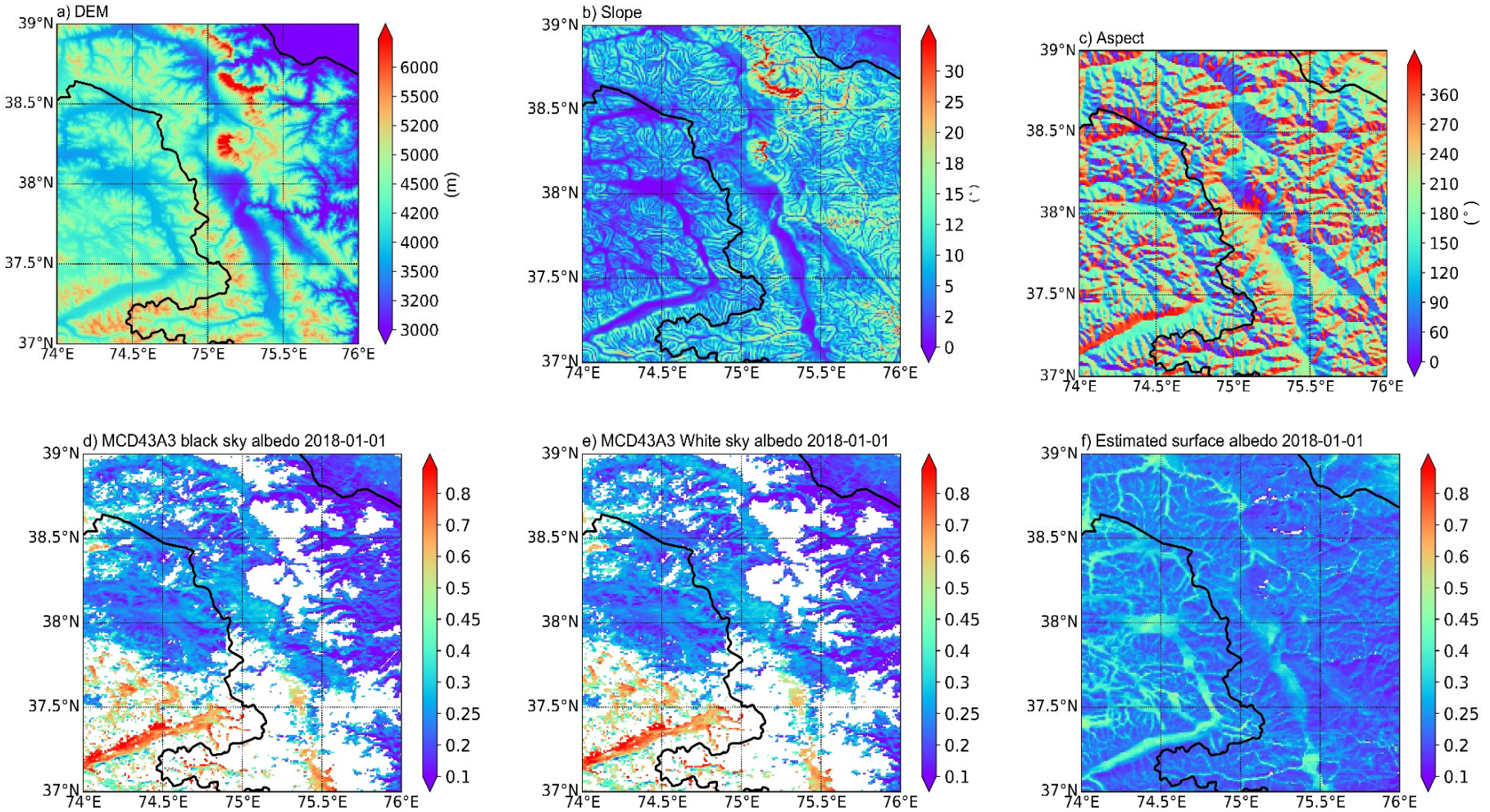


Mean cloud cover = 53%

mean AOD = 0.047

Spatio-temporal coverage of all-sky albedo

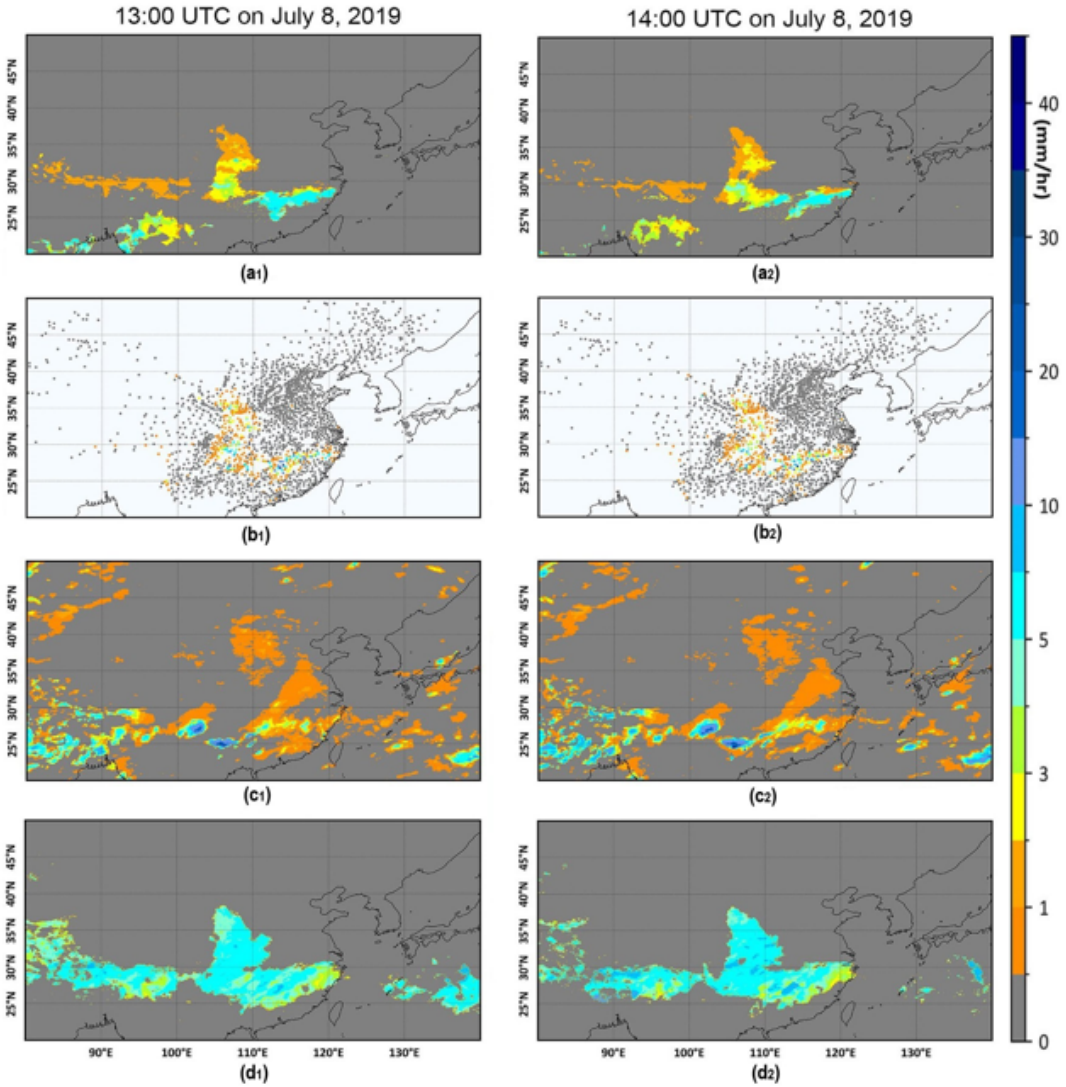
-Jia et al., 2024



- Spatial coverage much better than MCD3A3
- Correct association with landforms of retrievals below cloudy pixels

Overview of Chinese YSs research

Estimation of hourly precipitation with HIMAWARI data



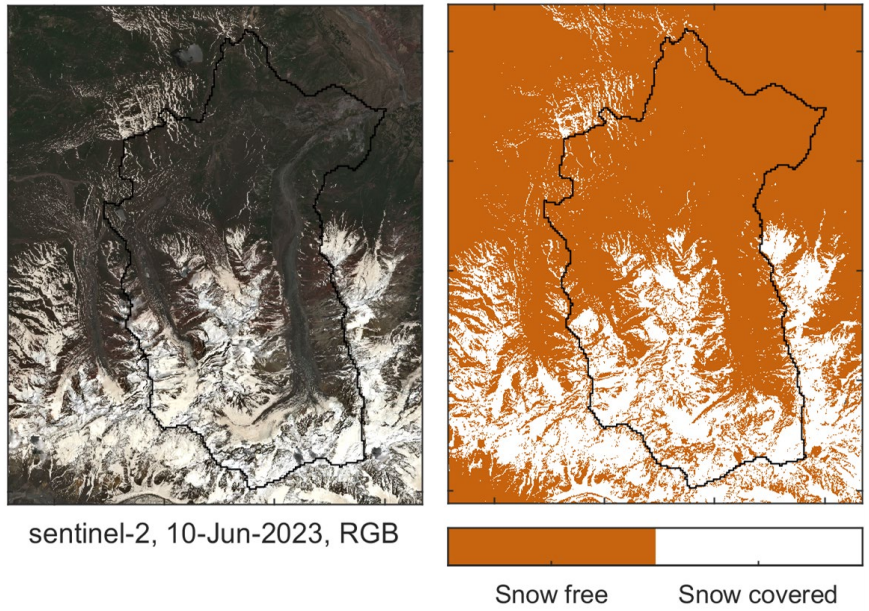
Hourly precipitation at 13:00 UTC (left panel) and 14:00 UTC (right panel) on July 8, 2019:

(a1, a2) D-PRA Estimates;
(b1, b2) Rain Gauge Observations;
(c1, c2) GSMaP_NOW Estimates;
(d1, d2) Fixed-variables Estimates.

(Cui et al, 2025 IEEE TGRS under review)

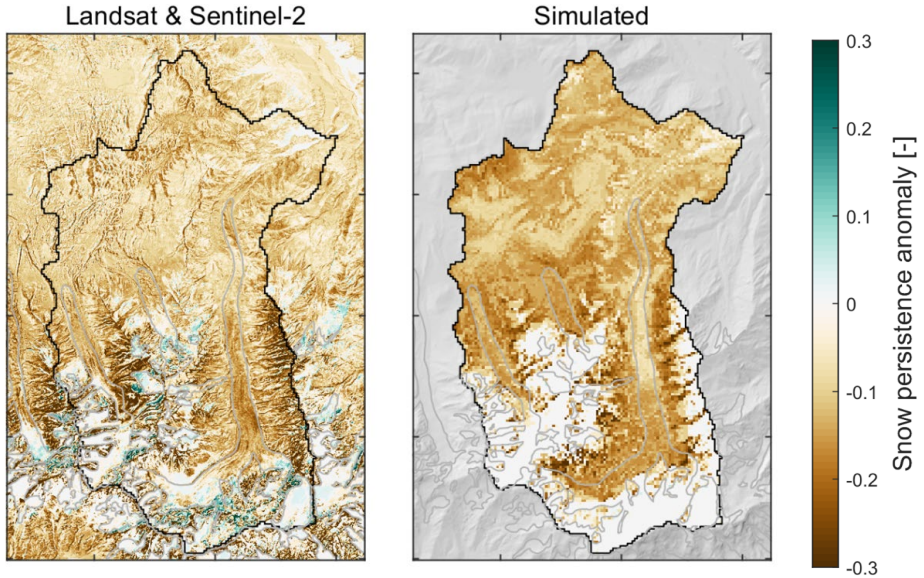
Temporal and spatial variability of snow cover

How is snow changing seasonally and long-term?



- Combining surface albedo and NDSI to map snow cover at high elevations
- Applied to multiple satellite surface reflectance products **(Landsat-5/7/8/9, Sentinel-2)**

Jouberton et al. in review

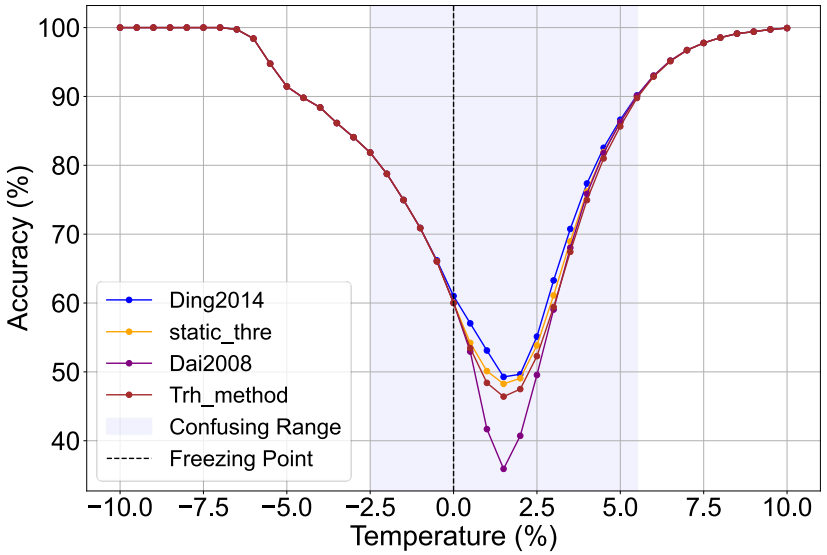


2018-2023 vs 2000-2018

- Multi-temporal snow cover maps allow to detect changes in snow persistence
- Remotely sensed snow cover changes can confirm similar changes derived from model simulations

Precipitation Phase Discrimination in China

Introduction



static_thre: fixed threshold = 0.6°C. **Ding2014**: Ding et al., 2014. **Dai2008**: Dai, 2008.**Trh_method**: Harder & Pomeroy, 2013.

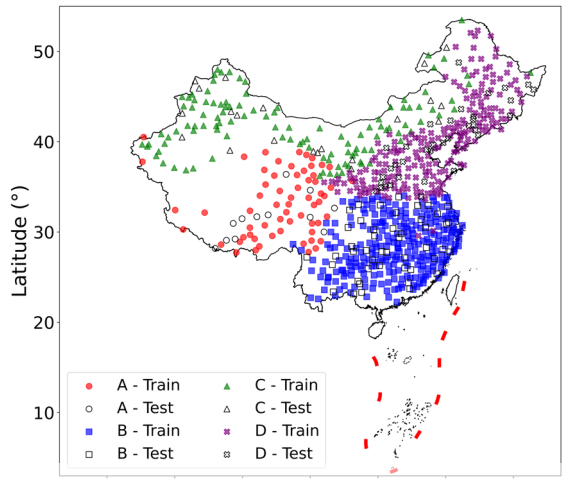
For Precipitation Phase Discrimination, accuracy of conventional methods commonly **drops below 90% between –7°C and 10°C, especially near 1°C**, even for best-prefroming Ding2014.

Data & Method

Daily Surface Climate Variables of China

Pre-processing & Quality Control

Divided into 4 regions based on elevation, January T_a, annual prec



In each region, 15% of stations are randomly used as test set

Considering sub-freezing rainfall events

Abnormal Standard:

T_a(rain) < **-5.4°C**; T_a(snow) > **8°C**;

T_a(sleet) < **-1.6°C** OR T_a(sleet) > **9.6°C**

Objective:

Constructing ML decision-tree or network from geo & meteorological info to precipitation phase

input: longitude, latitude, altitude (geo) wind, Ta, Relative humidty, pressure, precipitation amount(meteo); Tw, Td(calculated)

?

rain

sleet

snow

Five ML methods are explored:

SVM (Support Vector Machines) ;

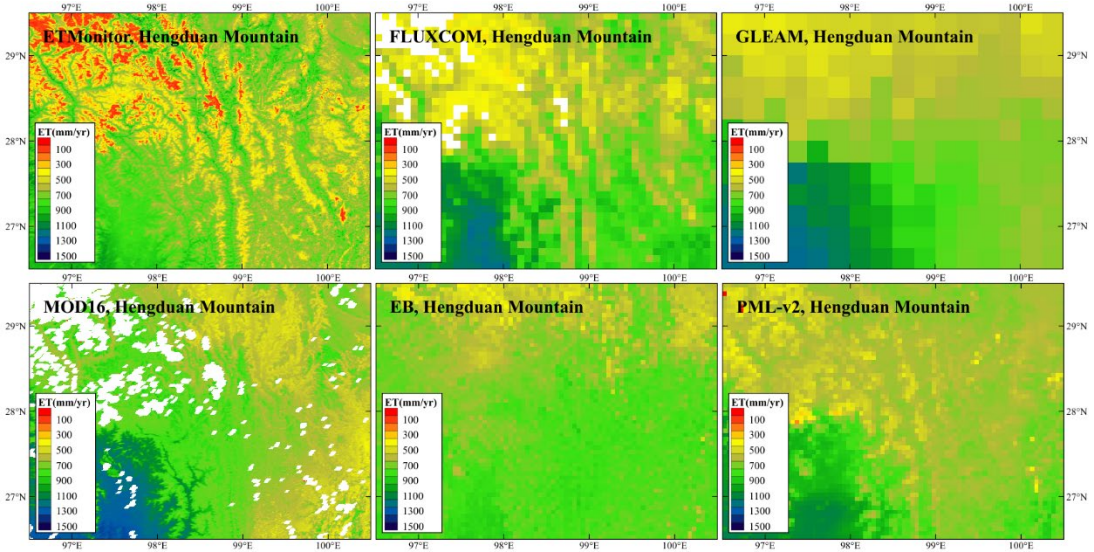
RF (Random Forest) ;

CatBoost (a gradient boosting algorithm) ;

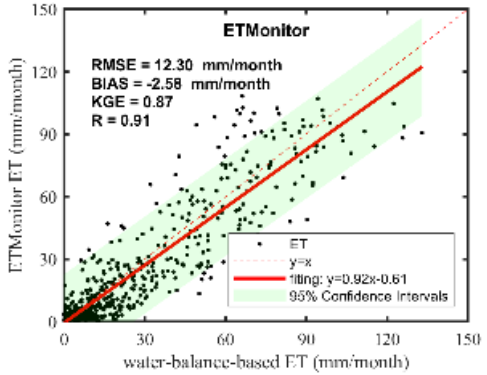
MLP (Multilayer Perceptron) ;

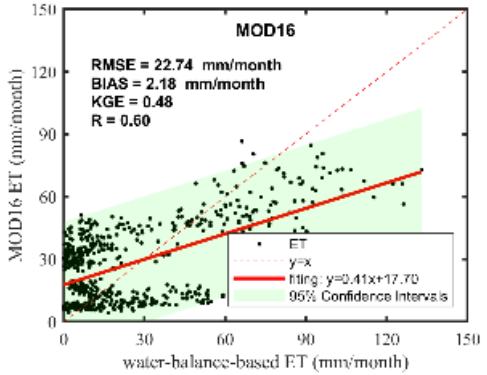
CNN (Convolutional Neural Network)

Vapour flux and its components

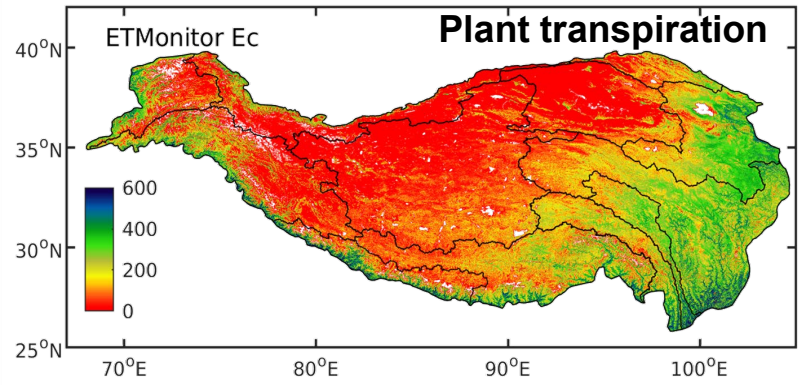


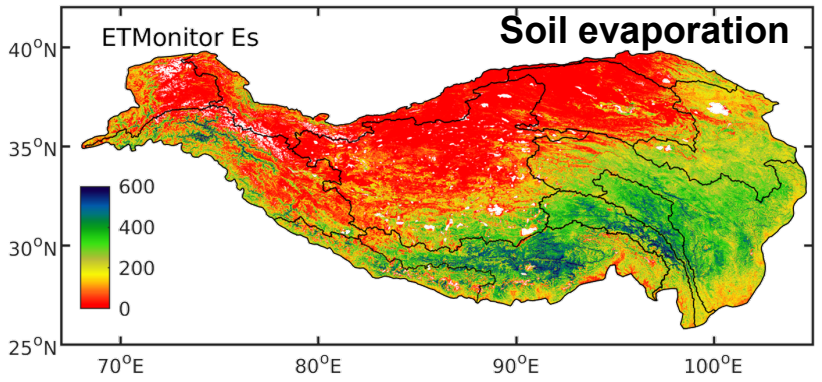
Spatial distribution of total vapour flux according to different data products Southeastern edge of the Tibetan Plateau (white pixels denote “no data”)

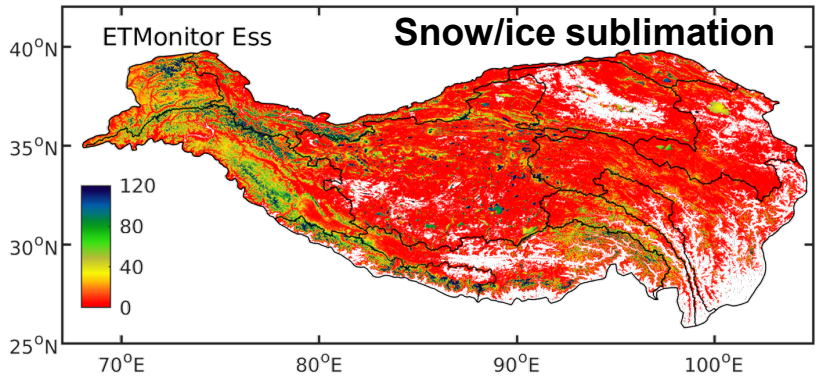




Validation of high-resolution data products against flux tower measurements







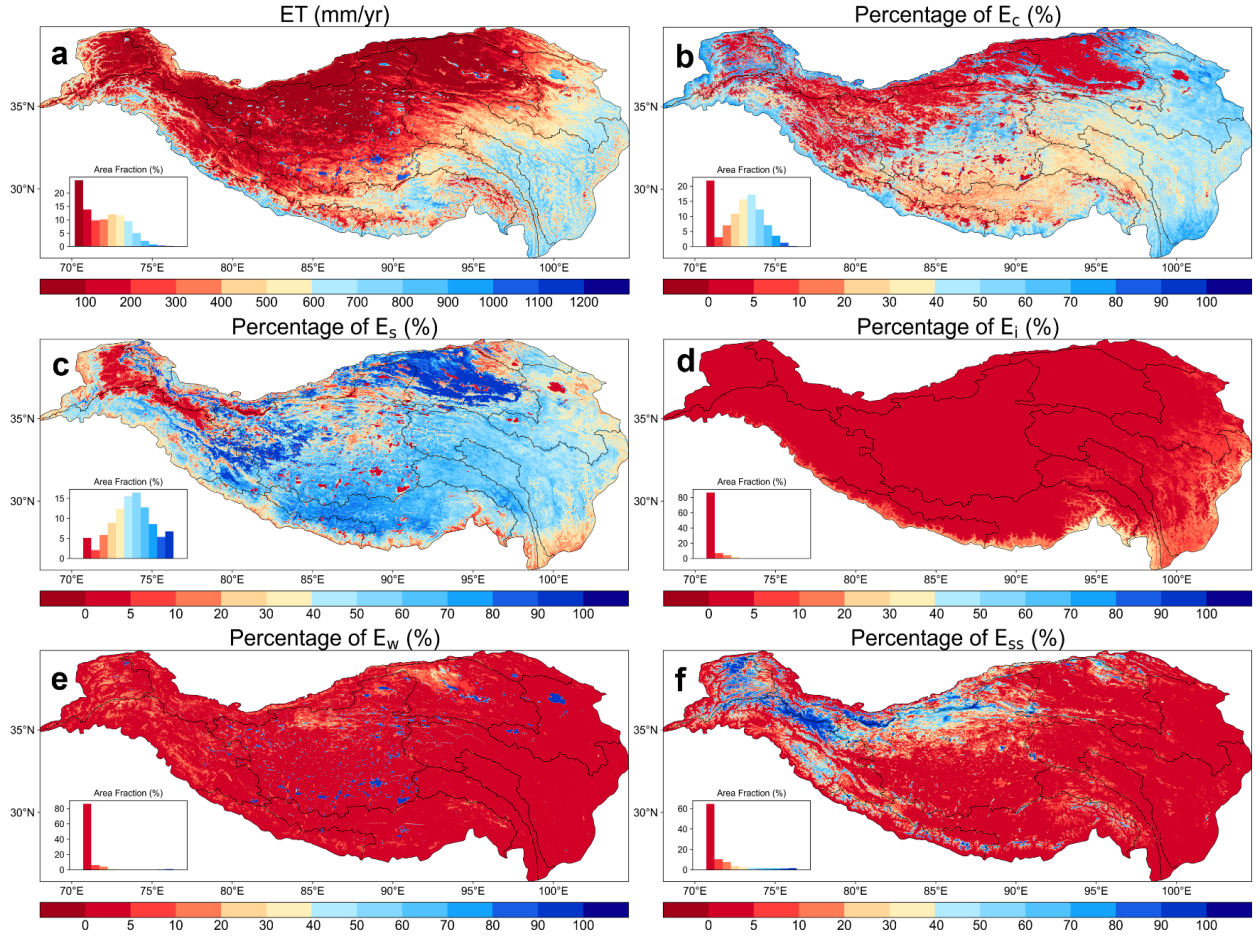
Zheng et al., 2023 J.Hydrol.; 2025 HESS

Vapour flux in the Tibetan Plateau

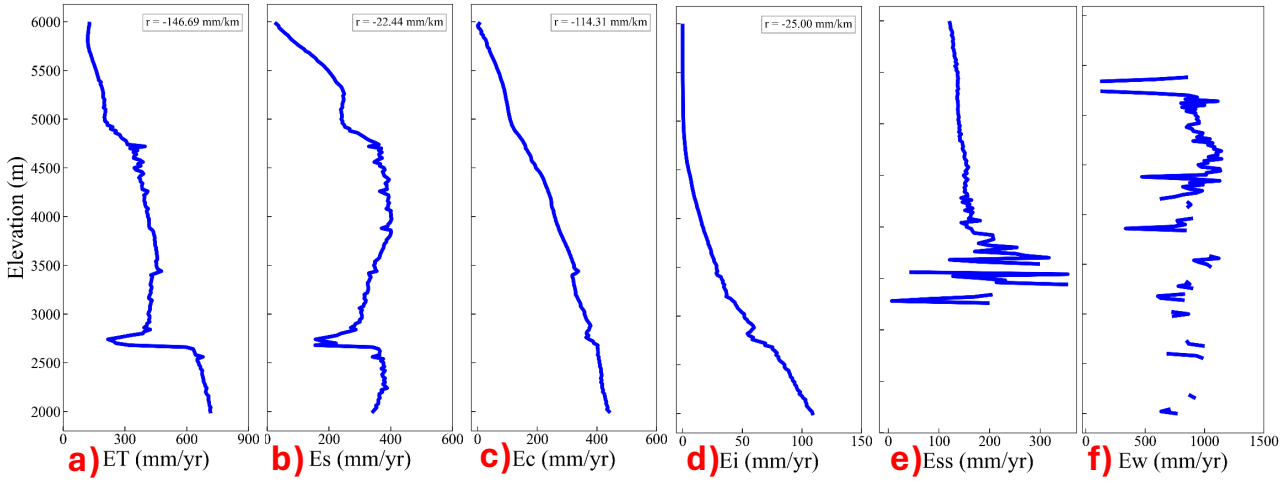
Water flux VS. DEM in TP

- **Total vaour flux decreases with increasing elevation (rate = 146mm/km), similar as transpiration (rate = 114mm/km)**

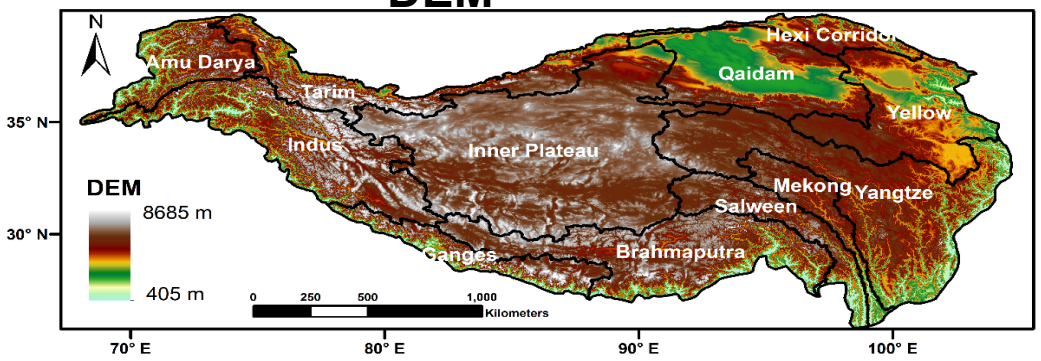
Vapour flux components by ETMonitor



Vapour flux components vs. elevation



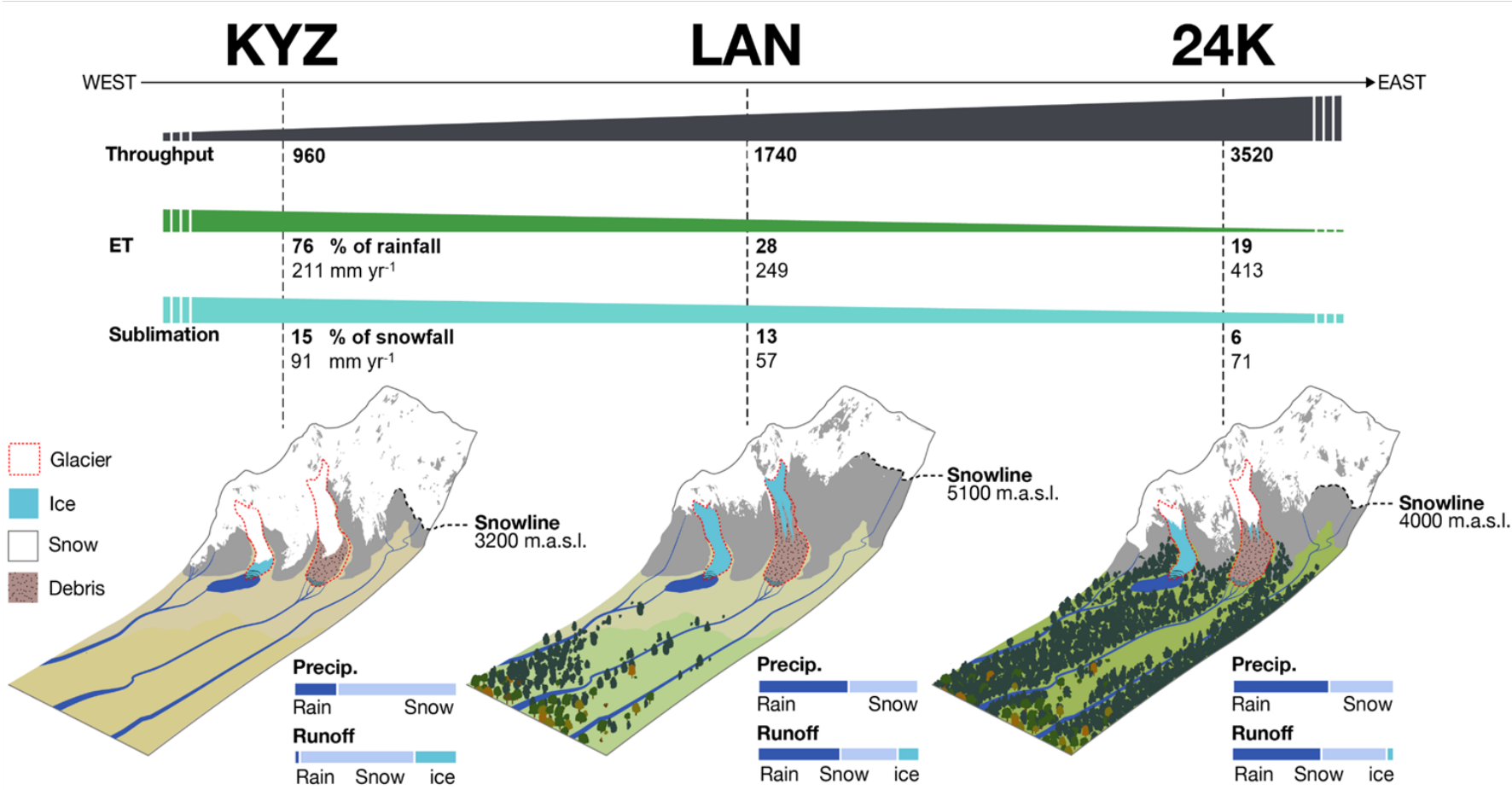
DEM



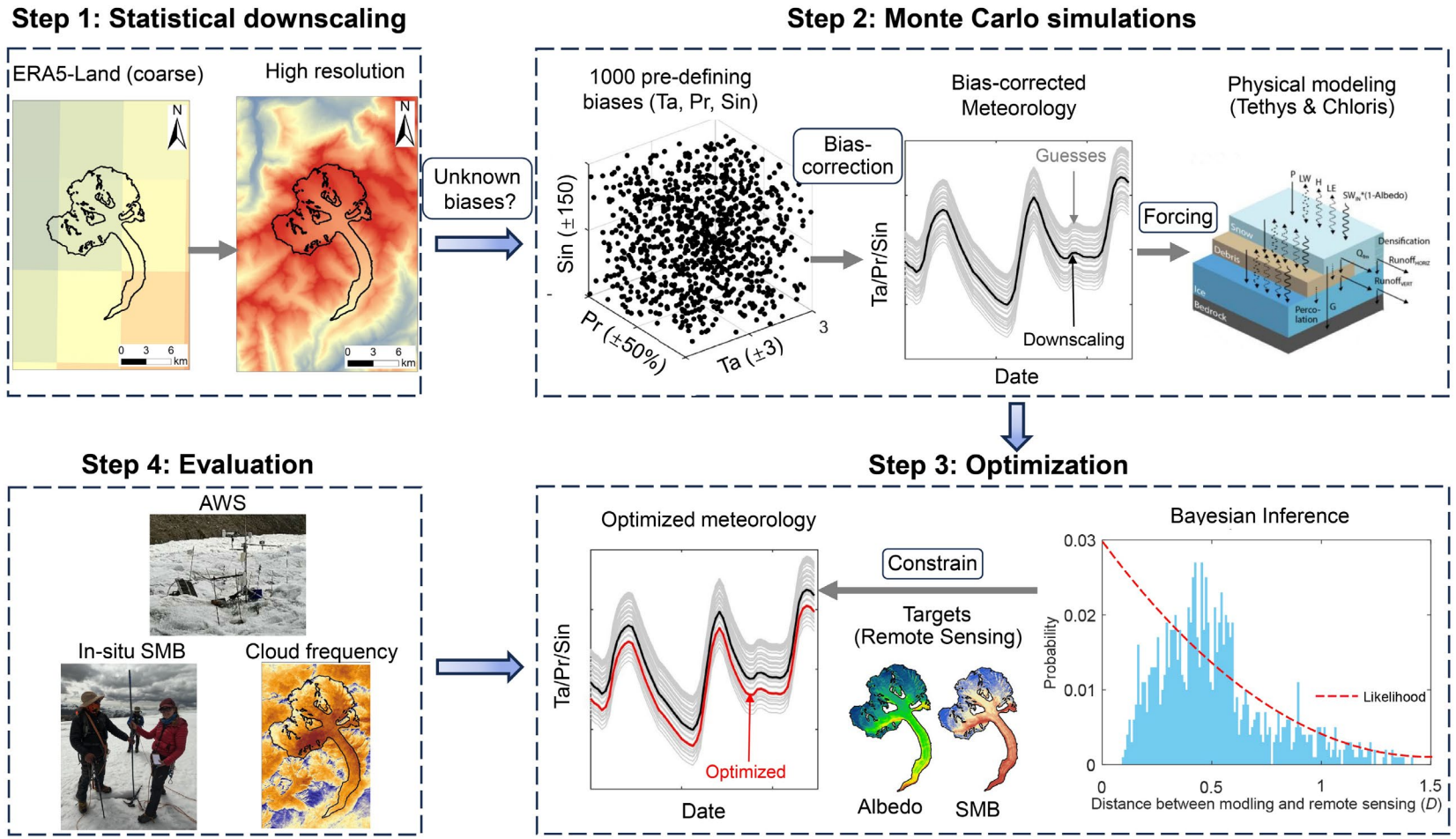
Ecohydrological modelling

- Sublimation removes 15%, 13% and 6% of snowfall
- Evapotranspiration removes 76%, 28% and 19% of rainfall

Fugger et al. 2024, ERL



Glacier meteorology inference



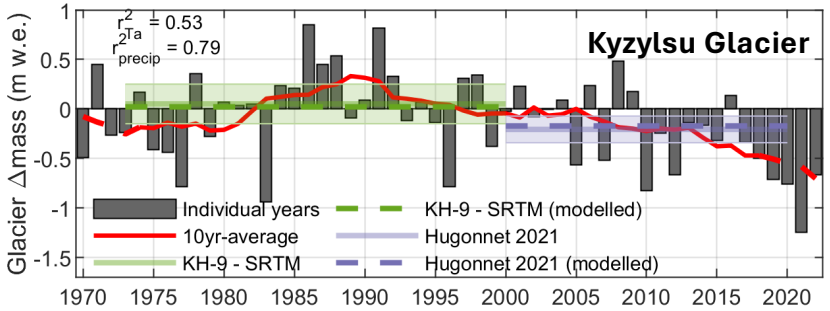
Concept:

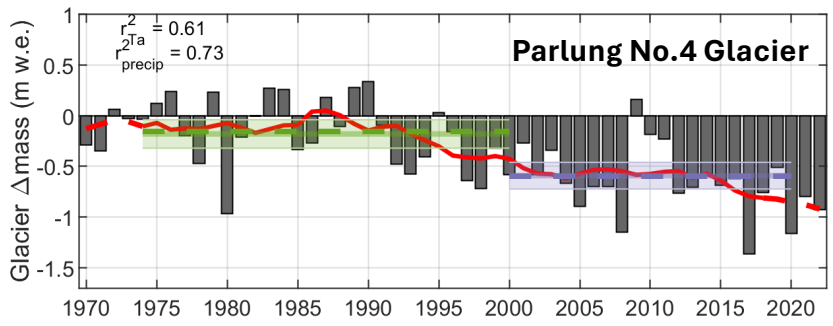
1. Statistical downscale
2. Monte Carlo model simulations
3. Bayesian inference against ***satellite albedo and mass balance***
4. Evaluation against local measurements

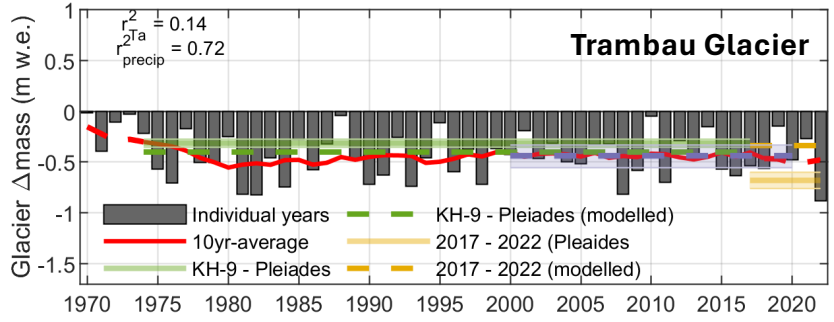
High elevation cryospheric and hydrologic processes

Results

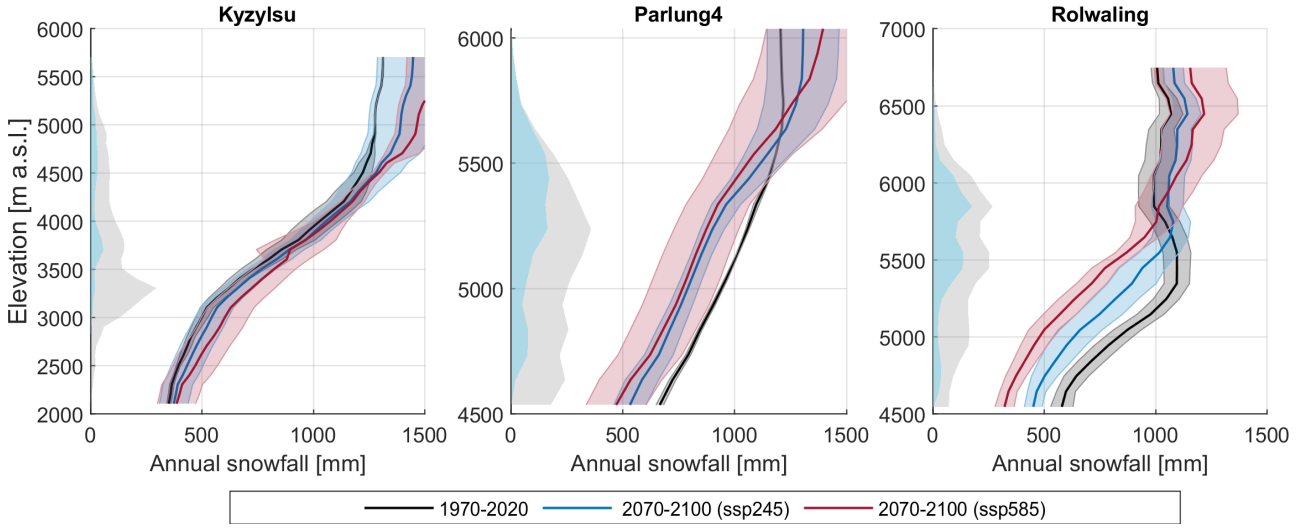
① Glacier mass changes since 1970



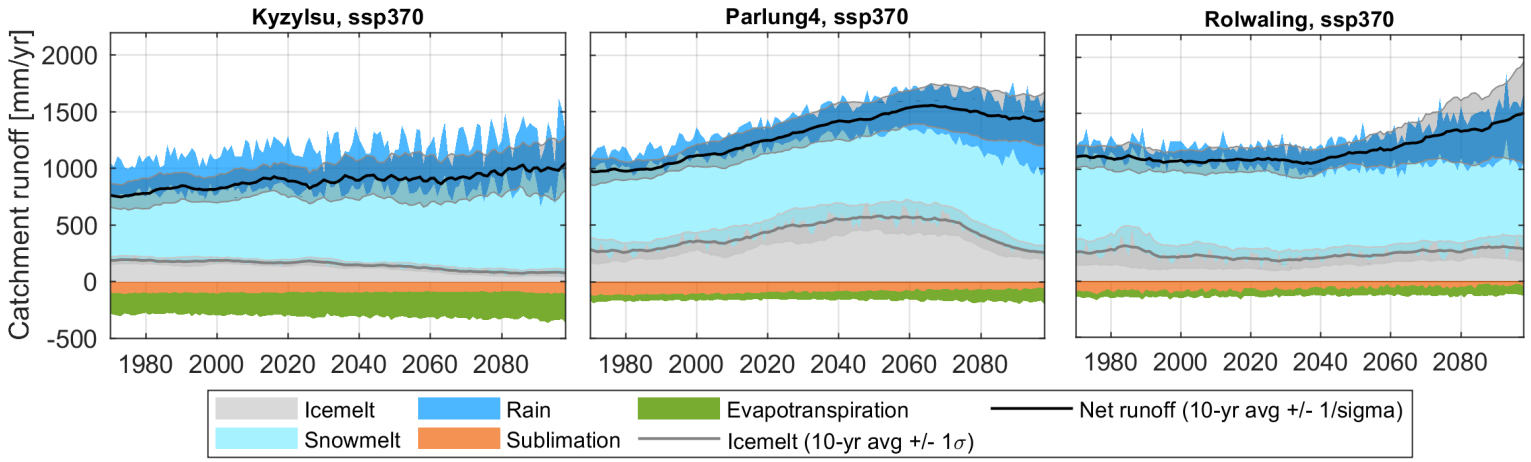




② Projected snowfall by 2100, per elevation band



③ Projected runoff until 2100



Concluding remarks



- Understanding the terrestrial water cycle in high elevation catchments is inherently multi-phase: water phases must be discriminated in water inflow, outflow and stocks
- Retrievals of glacier velocity and elevation changes in combination with surface albedo are the key to a better understanding of such processes
- A rich suite of spaceborne data is being exploited for this purpose
- First results confirm the feasibility of the approach to correct meteorological forcing data by inverse modelling of key properties of glacierized catchments
- Process models are being applied to assess response of the terrestrial water cycle in high elevation catchments to projected climate

Dragon 6 EO Data Delivery

Data access (list all missions and issues if any). NB. in the tables please insert cumulative figures (since June 2024) for no. of scenes of high bit rate data (e.g. S1 100 scenes). If data delivery is low bit rate by ftp, insert “ftp”

ESA /Copernicus Missions	No. Scenes
1. Sentinel-1	200
2. Sentinel-2	3000
3.	
4.	
5.	
6.	
Total:	3200
Issues:	

ESA Third Party Missions	No. Scenes
1. Landsat 5, 7, 8 and 9	2000
2. PlanetScope	200
3. SPOT 6/7 mono	6000 km2
4. SPOT 6/7 tri-stereo	1500 km2
5. Pleiades bi-stereo	10000 km2
6.	
Total:	2200 + 17500 km2
Issues: _note: all data listed above have been accessed through other projects; this does not include the Dragon-6 allocation	

Chinese EO data	No. Scenes
1. GF-1 WFV	48
2. GF-6 WFV	3
3. SDGSAT-1	10
4.	
5.	
6.	
Total:	61
Issues: _have not seen data access specifications from ESAs	

European Young Scientists contributions in Dragon 6

Name	Institution	Poster title	Contribution including period of research
Achille Jouberton	ISTA	ID 238 Modeling the water balance of selected glacierized catchments in High Mountain Asia from 1970 to 2100	Analysis of snow cover variations and vegetation phenology from EO data (WP1); Forward modelling of glacierized catchments using hyper resolution ecohydrological model (WP3); 2024-present
Haruki Hagiwara	ISTA	ID 237 Quantifying Glacier Mass Change in the Western Pamirs (2003–2024): Insights from High-Resolution DEM Time Series	Analysis of stereo satellite data for DEM and orthoimage production and glacier thickness change measurement (WP1); 2024-present
Shaoting Ren	ISTA	ID 236 Recent Response Of Pamir Glaciers To Intensified Global Warming	Analysis of multispectral satellite data for determination of albedo and surface temperature variability (WP1); Inverse modelling with hyper-resolution model to infer climate reanalysis biases (WP2); 2024-present
Stefan Fugger	ISTA	Not attending. Completed employment.	Analysis of vegetation phenology from EO data (WP1); Forward modelling of glacierized catchments using hyper resolution ecohydrological model (WP3); 2024
Juan Melo Velasco	ISTA	Not attending.	Forward modelling of glacierized catchments using hyper resolution ecohydrological model (WP3); 2024-present

Chinese Young Scientists contributions in Dragon 6

Name	Institution	Poster title	Contribution including period of research
Jiu CHEN	AIR - CAS	158 Estimate Accurate Glacier Flow Velocity with Appropriate Temporal Baseline	Development of methods; data processing and analysis; 2024 - 2025
Mengyuan CUI	AIR - CAS	Hourly precipitation China / highlight Tibet	Development of methods; data processing and analysis; 2024 - 2025
Wangkan SHE	Tsinghua University	Machine Learning-Based Methods for Precipitation Phase Discrimination in China	Development of methods; data processing and analysis; 2024 - 2025



Monitoring seasonal accumulation in high-elevation catchments

Haruki Hagiwara

WP1: Ice and snow volume changes

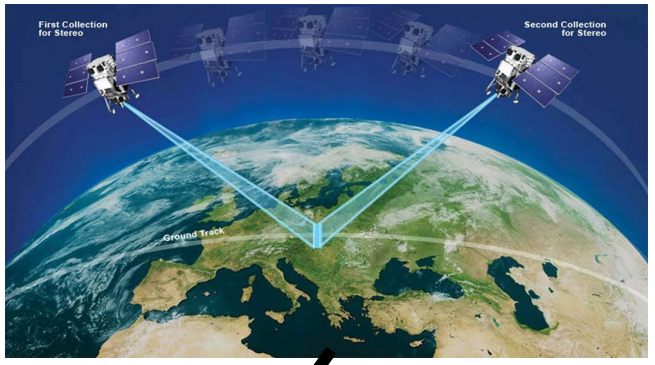
Monitoring seasonal accumulation in high-elevation catchments

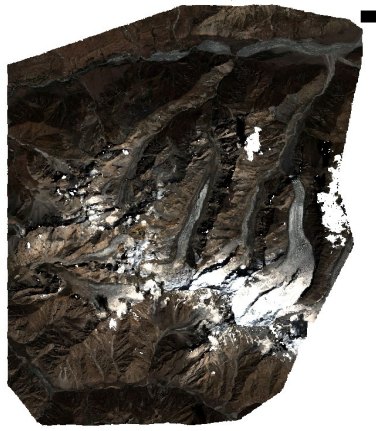
Method

Compare surface Digital Elevation Models (DEMs) by high-resolution Pléiades stereo satellite imagery

Pléiades (CNES, AIRBUS)

- 0.5m resolution
- < 1m vertical precision



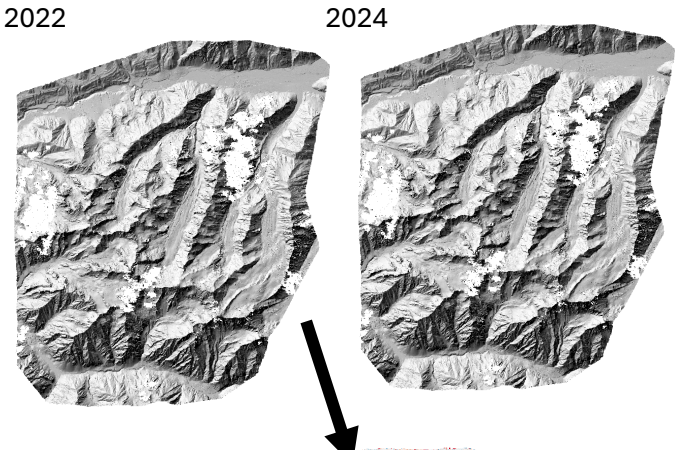


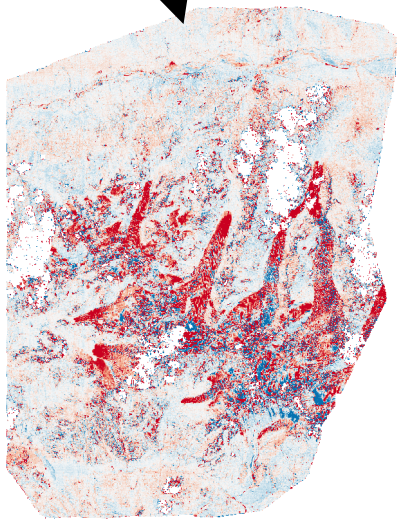


DEM

2022

2024





Elevation change

WP1: Ice and snow volume changes

Monitoring seasonal accumulation in high-elevation catchments

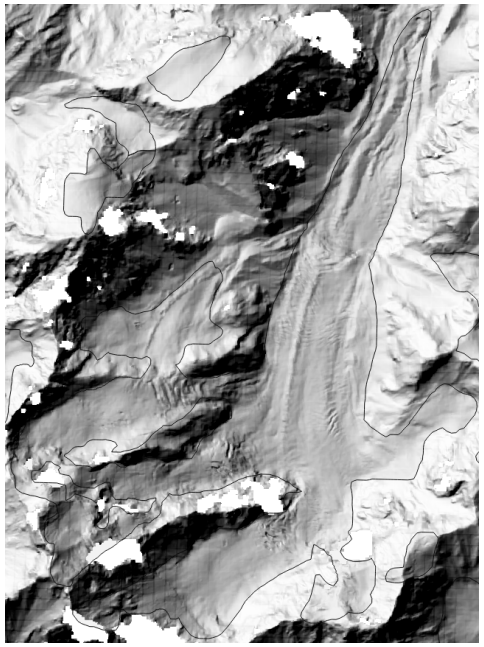
Method

Compare surface Digital Elevation Models (DEMs) by high-resolution Pléiades stereo satellite imagery

Pléiades (CNES, AIRBUS)

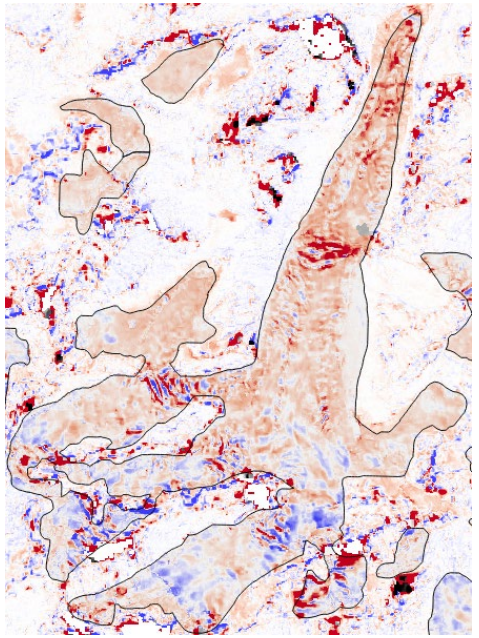
- 0.5m resolution
- < 1m vertical precision

DEM

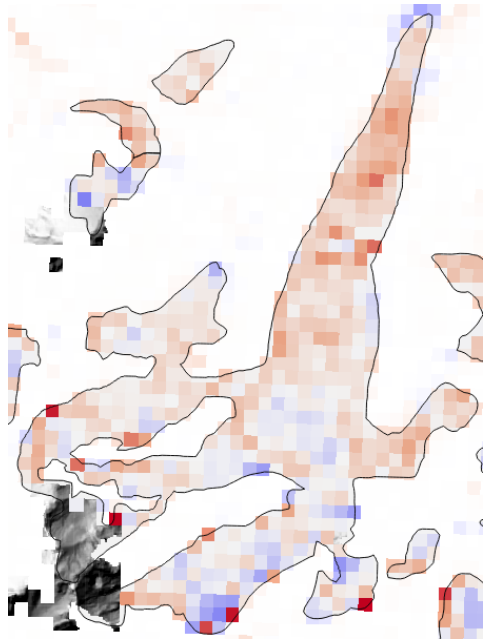


2m resolution (Pléiades)

Elevation change



2m resolution (Pléiades)

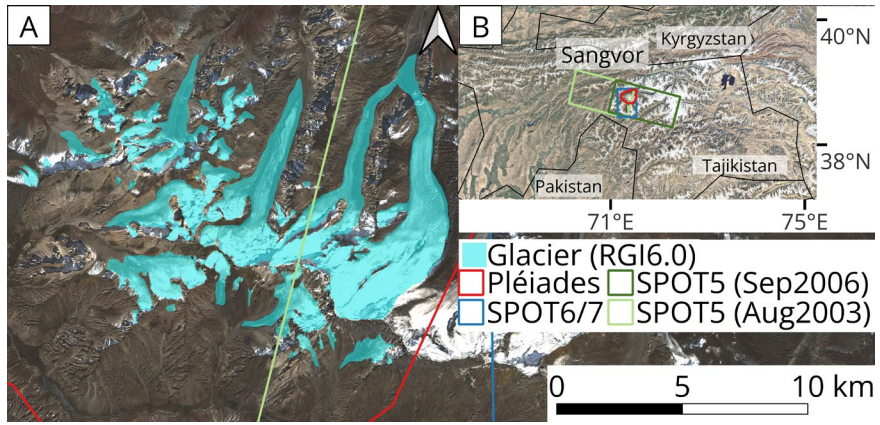


30m resolution (ASTER)

- **Assess the mass balance by satellites**
- **Disentangle interannual mass balance changes**

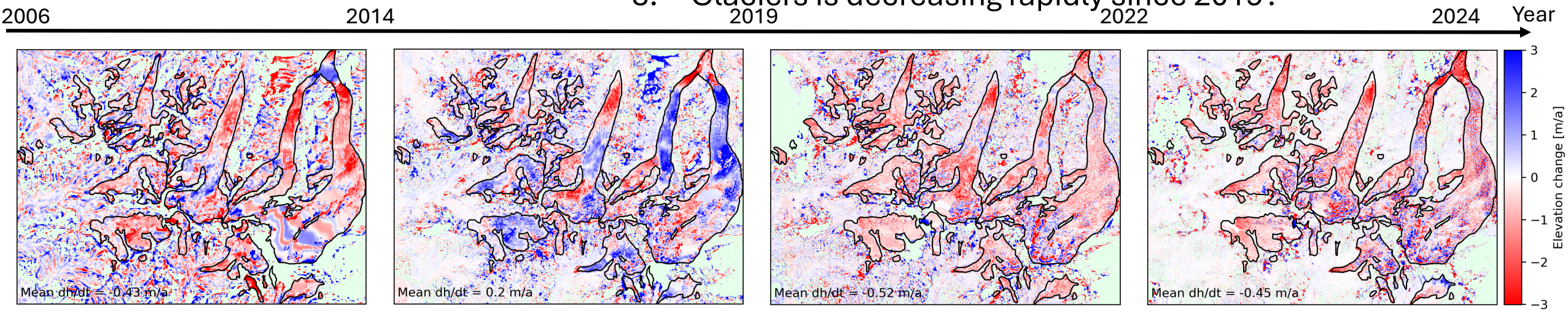
WP1: Ice and snow volume changes

Insights from high-resolution DEM time series



Study site: Sangvor, Tajikistan

1. Surge event between 2006 and 2014?
2. Huge elevation gain between 2014 and 2019?
3. Glaciers is decreasing rapidly since 2019?



Mean dh/dt: -0.43 ± 0.15 [m/a]

Mean dh/dt: +0.2 ± 0.10 [m/a]

Mean dh/dt: -0.52 ± 0.18 [m/a]

Mean dh/dt: -0.45 ± 0.29 [m/a]

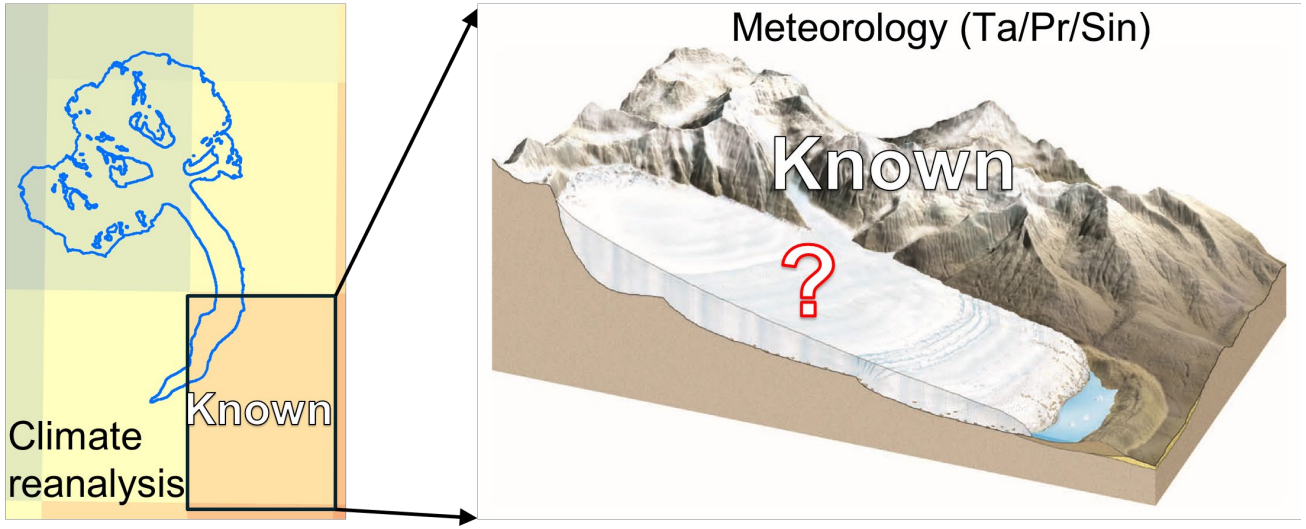


Glacier meteorology inference

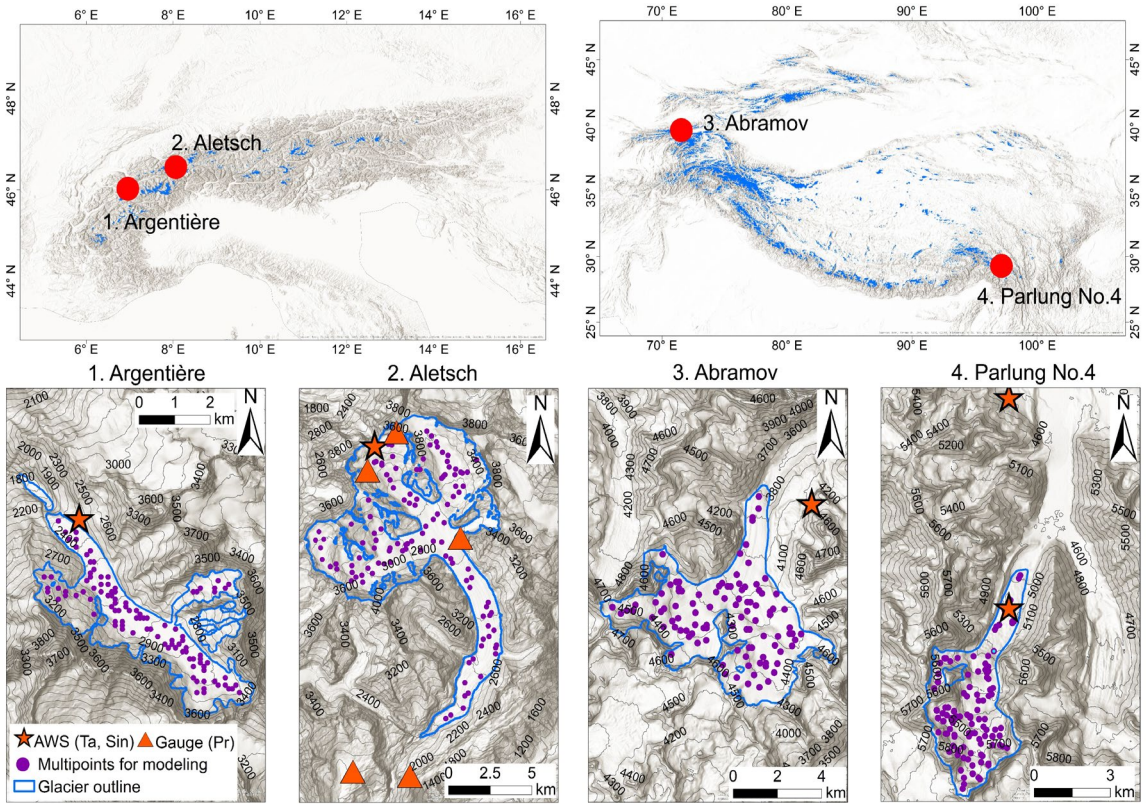
Shaoting Ren

Glacier meteorology inference

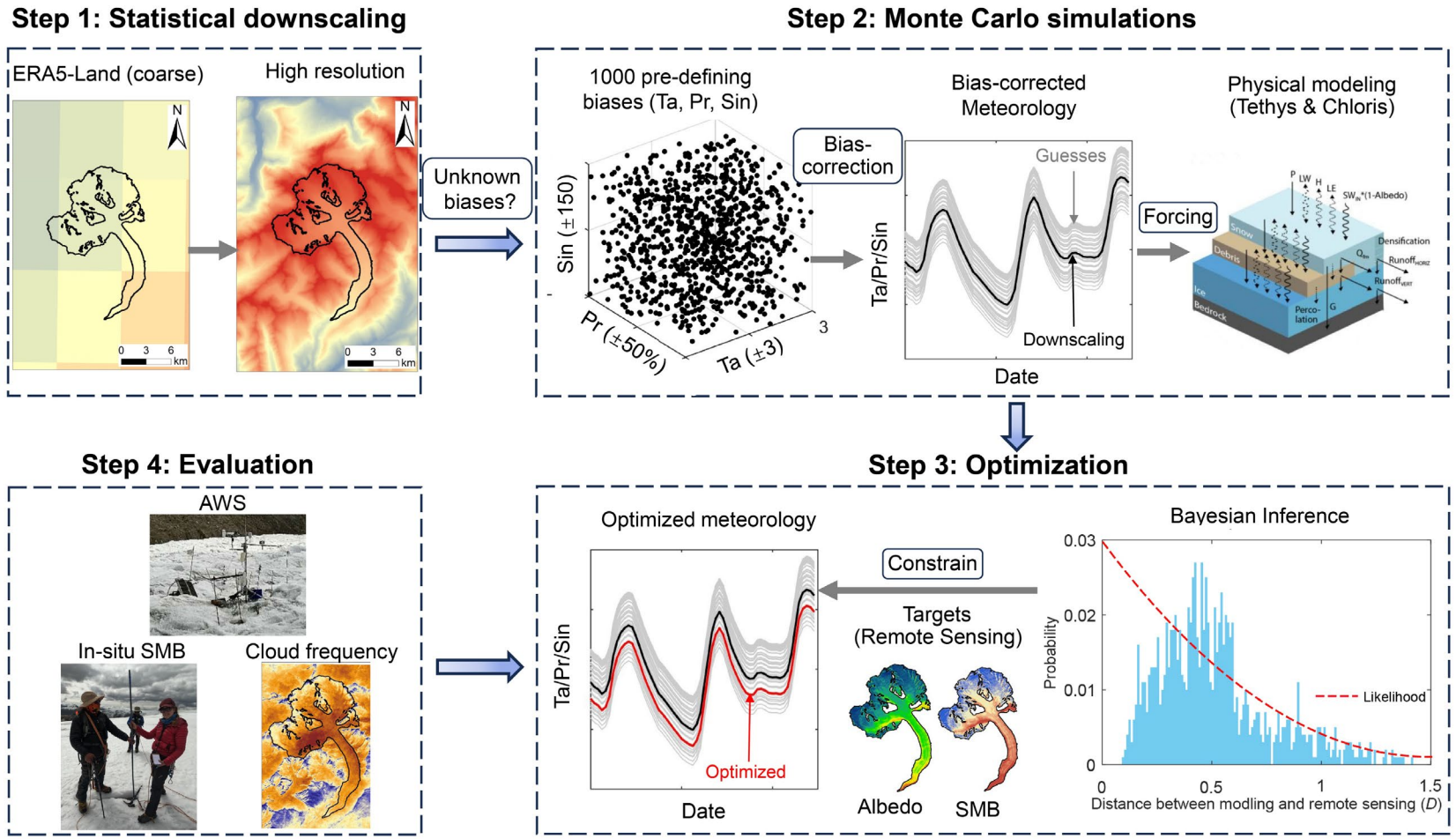
Challenge: Difficult to obtain glacier meteorology



Study sites



Glacier meteorology inference

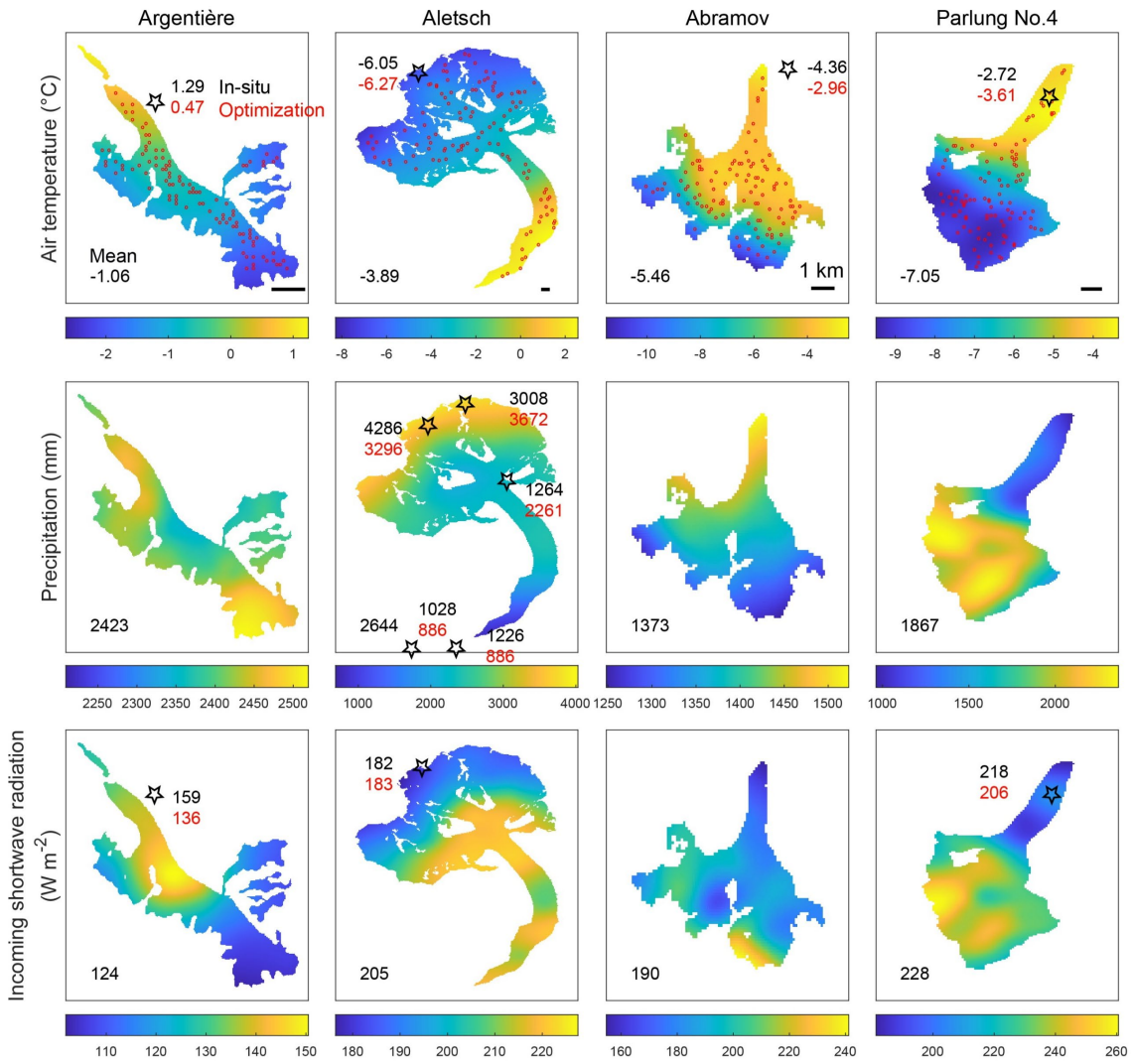


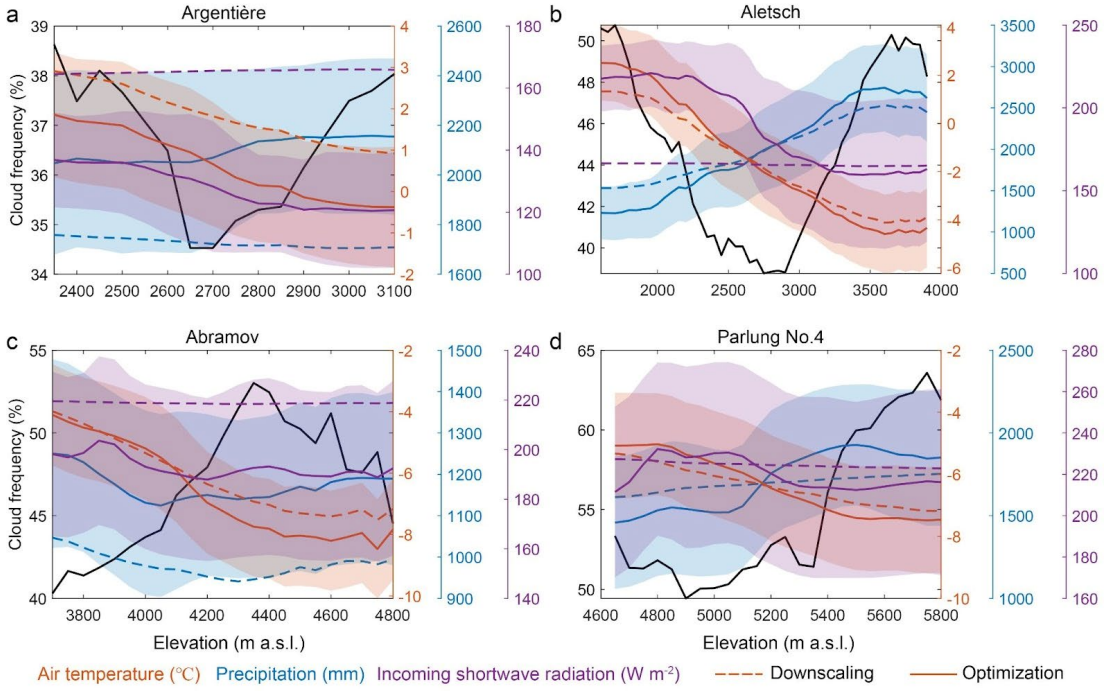
Concept:

1. Statistical downscale
2. Monte Carlo model simulations
3. Bayesian inference against ***satellite albedo and mass balance***
4. Evaluation against local measurements

IMMERSE (ID. 95462) WP2: Glacier meteorology inference

Spatial pattern of inferred glacier meteorology





Results:

1. Highly spatially variable
2. Better agreement with local measurements compared with downscaling

Glacier and runoff changes in glacierized catchments

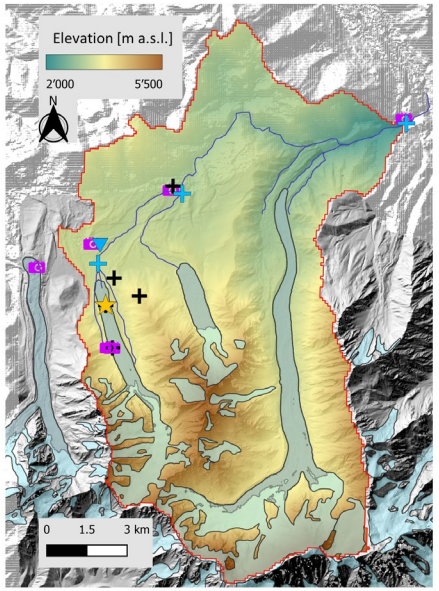
Achille Jouberton

Overview of European YSs research

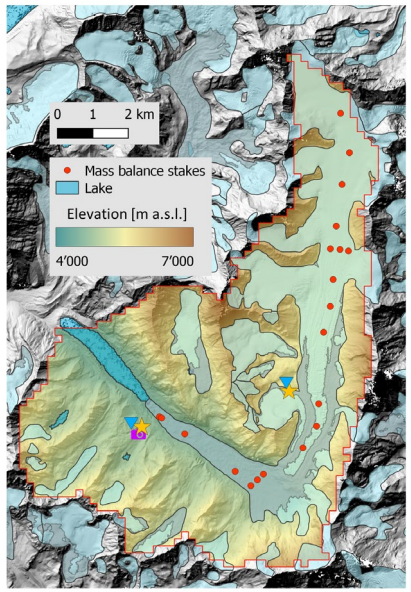
Fatichi et al. (2012)

Study sites

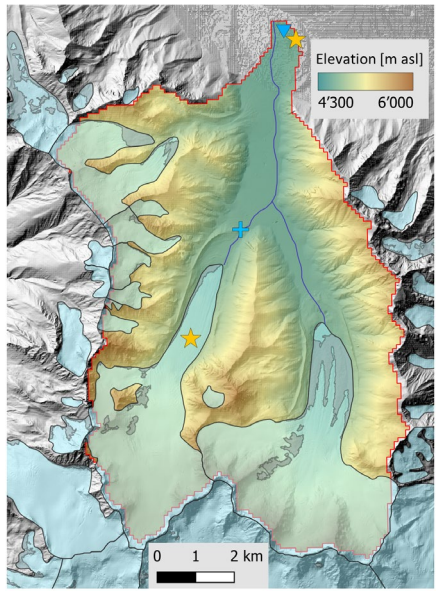
Kyzylsu, Tajikistan

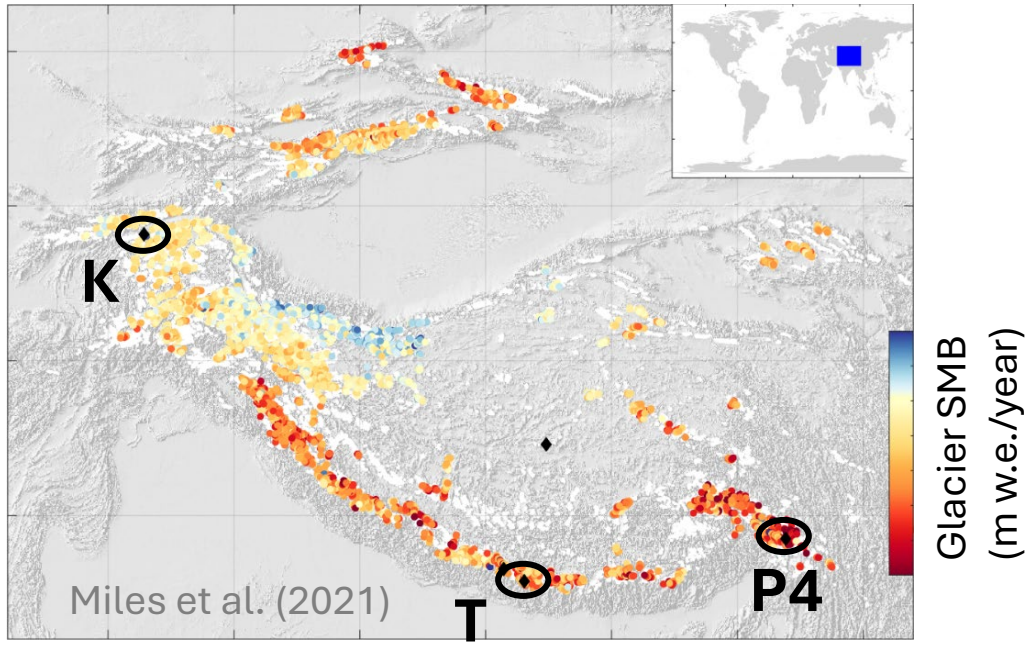


Trambau, Nepal



Parlung No.4, China



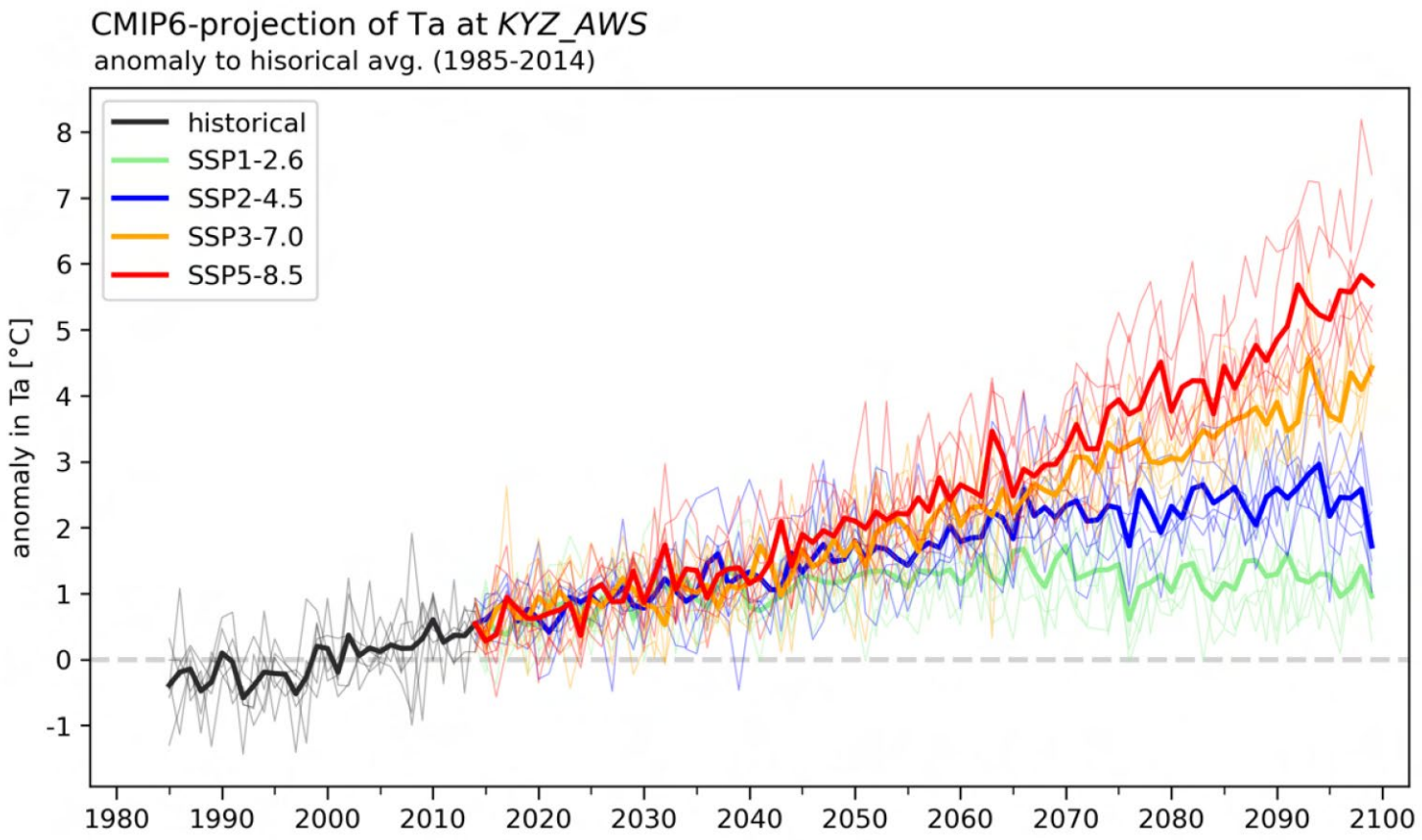


- Three benchmark catchments, with areas of 100 and 200 km^2, spanning elevations ranging from 2000 to 6500 m a.s.l.
- 3 to 10 years of hydro-meteorological measurement time series.

Overview of European YSs research

Future projections

- GCMs (General Circulation Models) from CMIP6.
- Select ~5 from 20 models available
- **Spatial resolution** : ~100 to 200km
- **Temporal resolution**: usually daily



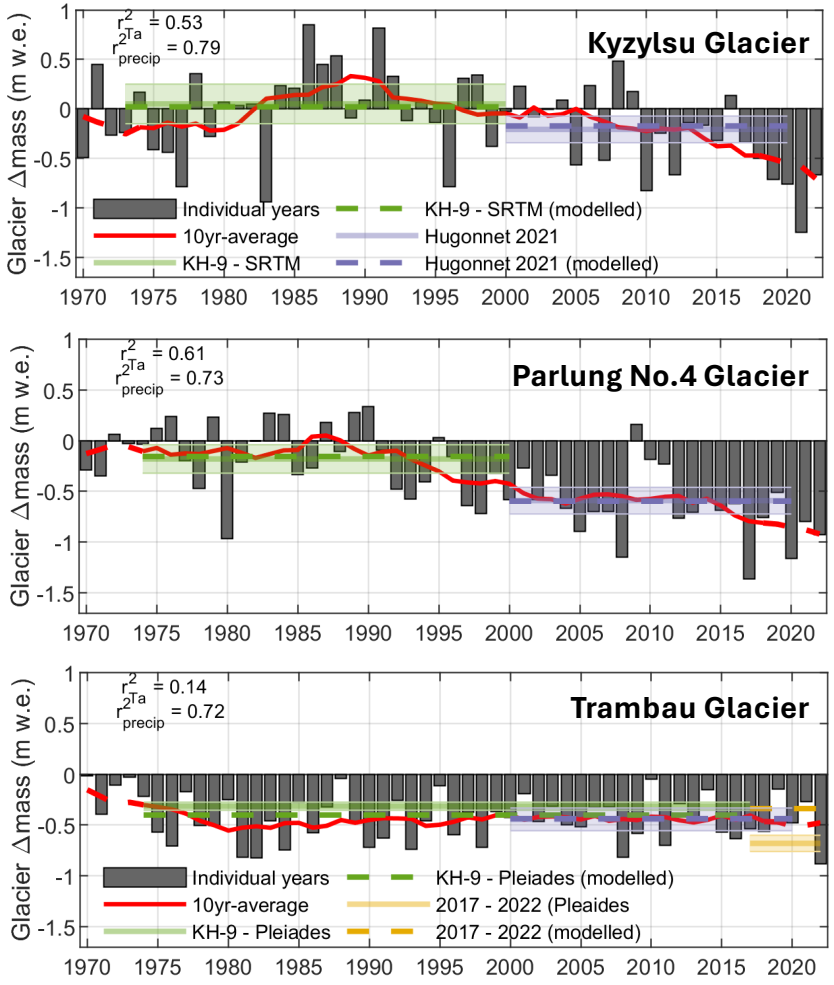
Statistical downscaling

- Empirical quantile mapping
- Disaggregated from daily to hourly using Melodist

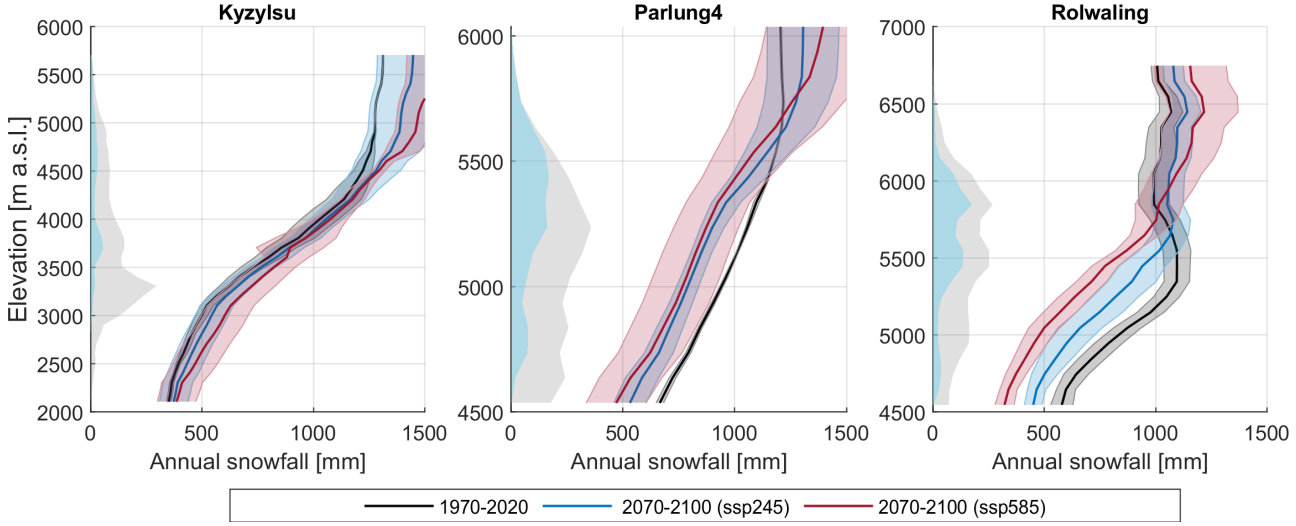
Overview of European YSs research

Results

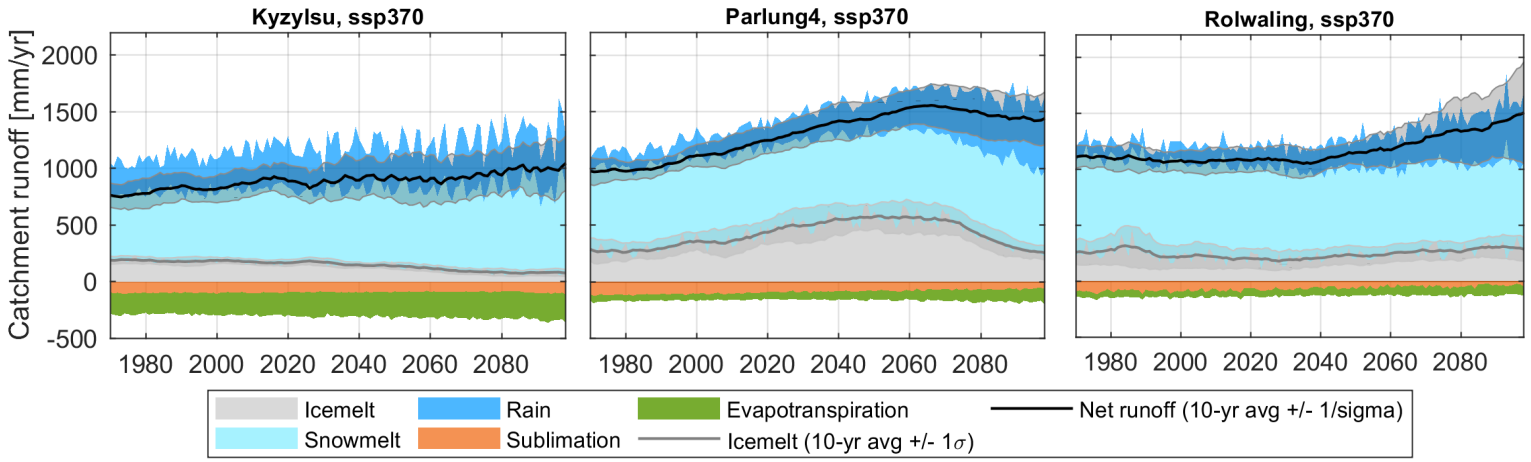
① Glacier mass changes since 1970



② Projected snowfall by 2100, per elevation band



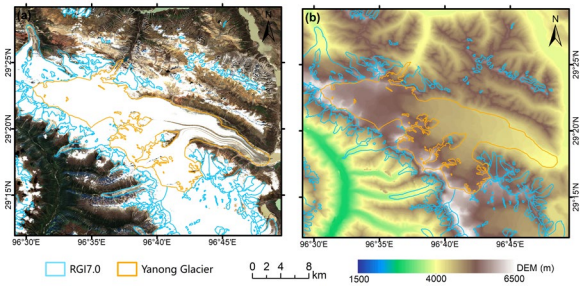
③ Projected runoff until 2100



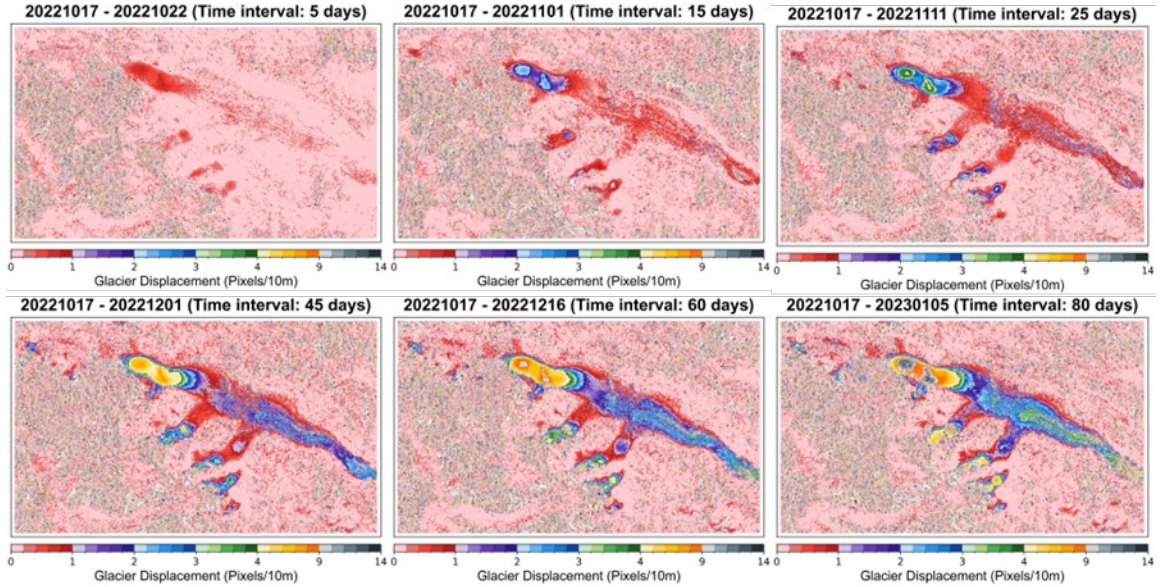
Estimate Accurate Glacier Flow Velocity with Appropriate Temporal Baseline

Jiu Chen

Optimal time intervals for optical image cross-correlation

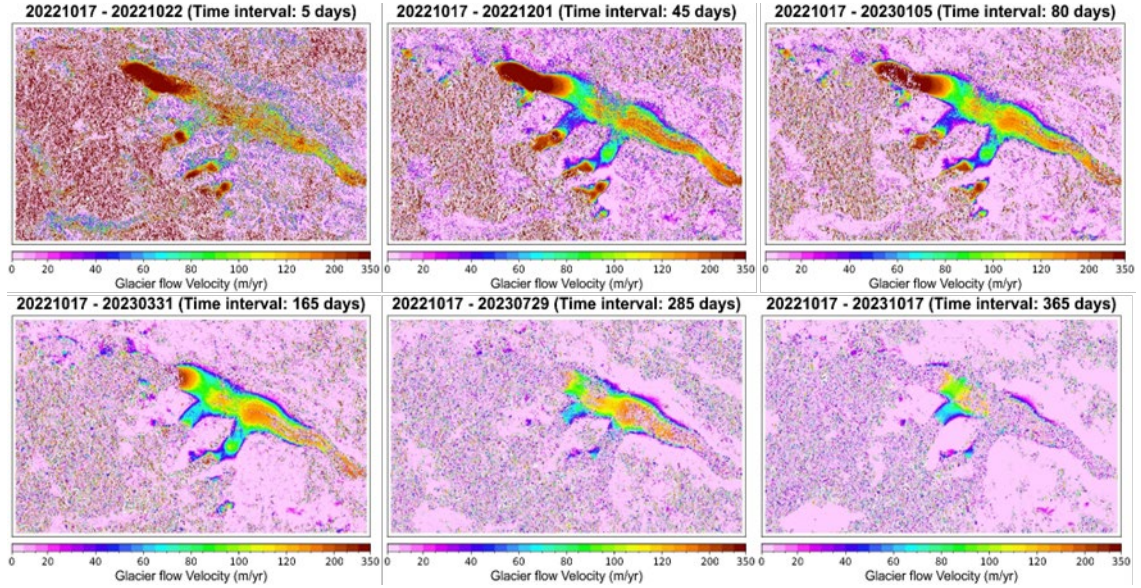


- **Study area**: Yanong Glacier in the southeastern Tibetan Plateau
- **Data**: Sentinel-2 MSI Products; **Method**: COSI-Corr
- The appropriate time interval: **45 and 120 days**
  - ✓ **Short time interval**: the displacement is too small to be detected
  - ✓ **Long time interval**: lose the correlation (the surface morphology of glaciers changes)



The glacier displacements

(Using image pairs with **different time intervals** and the **COSI-Corr** method)



The glacier flow velocities

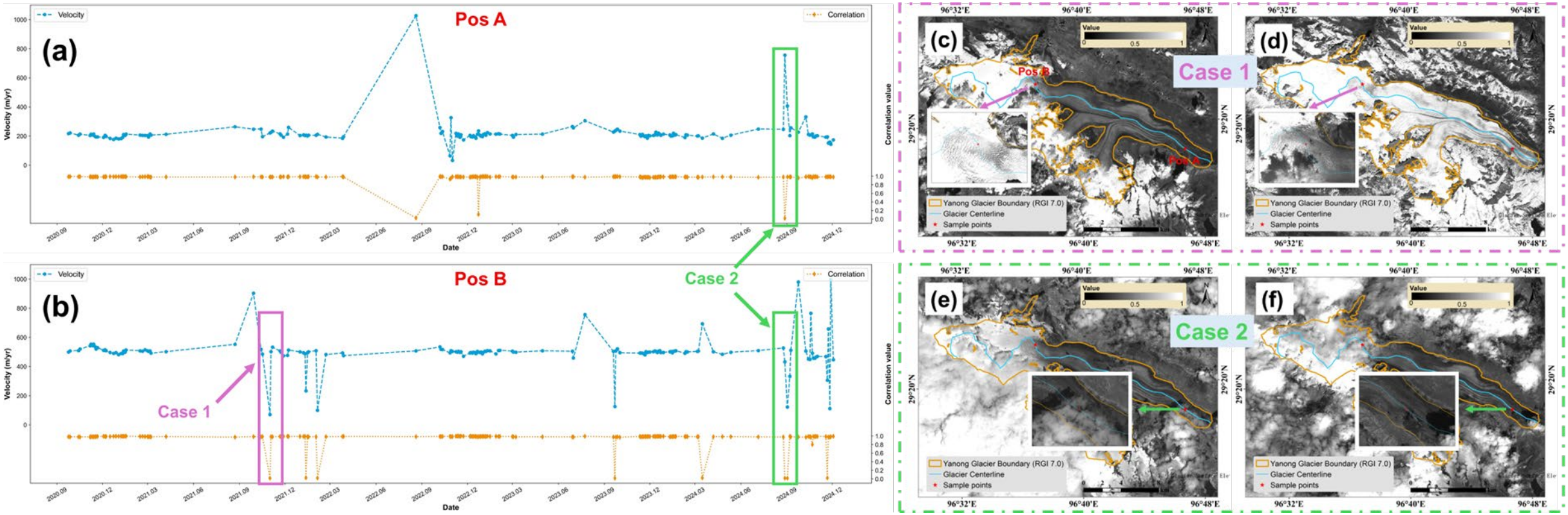
(Using image pairs with **different time intervals** and the **COSI-Corr** method)

(Chen et.al., 2025 manuscript)

Screening the outliers in the glacier flow velocity time series

(Chen et.al., 2025 manuscript)

- Select image pairs with a time interval between 45 and 60 days
- The date of the time series: the middle date of image pairs
- Outliers with low correlation values: **Snow cover (Case 1) ; Cloud cover (Case 2)**



Outliers in the glacier flow velocity time series with low correlation values

Time series of glacier flow velocities and their correlation values at Position A (a) and B (b);

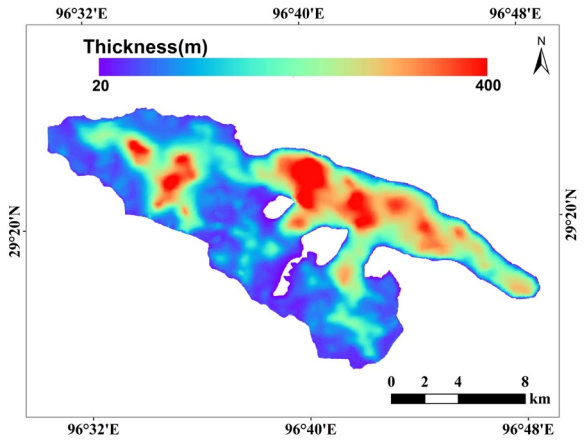
Sentinel-2 NIR map of Yanong glacier, on October 2, 2021 (c), December 1st, 2021 (d), August 2, 2024 (e) and September 21, 2024 (f) respectively

Use the continuity equation to get mass balance

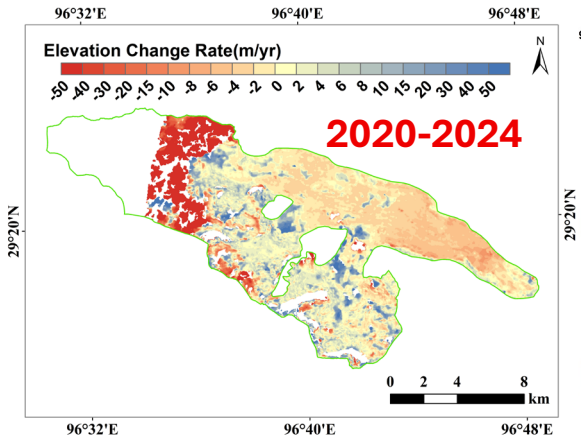
The continuity equation

$$b_s = \frac{\partial h}{\partial t} + \nabla \cdot q$$

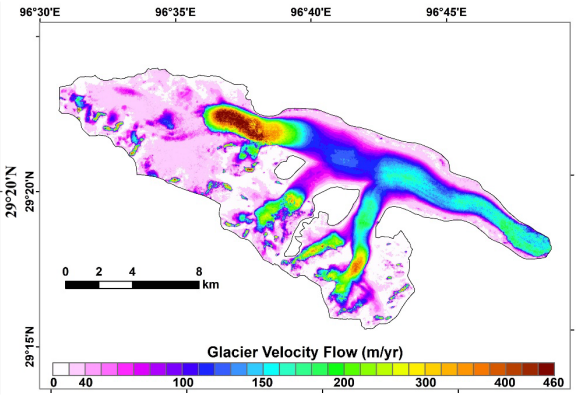
SMB — DEM Change — Ice flux



Thickness
(RGI6.0 Ice Thickness Model, 30m)

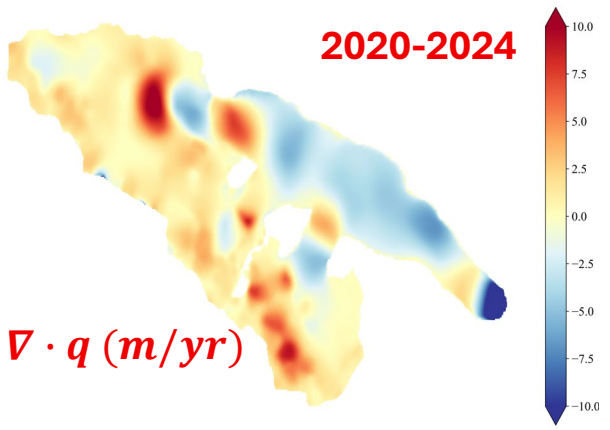


DEM changes
(Based on ASTER L1A image and MMSATER method, 30m)

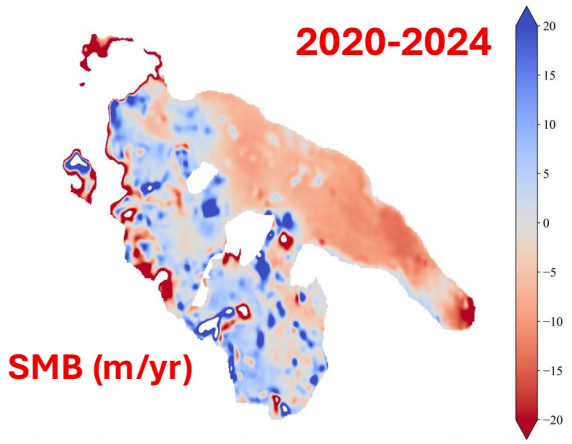


Flow velocity
(Based on Sentinel-2 MSI image and COSI-Corr)

- The ratio of **Ice Flux Divergence** to **Surface Mass Balance** is comparable (Ice Flux Divergence **MUST** be taken into account)
- **Glacial movement** is a key factor that cannot be ignored in the estimation of mass balance



Ice Flux Divergence



Surface Mass Balance

(Chen et.al., 2025 manuscript)

Estimation of hourly precipitation with HIMAWARI data

Mengyuan Cui

Overview of Chinese YSs research

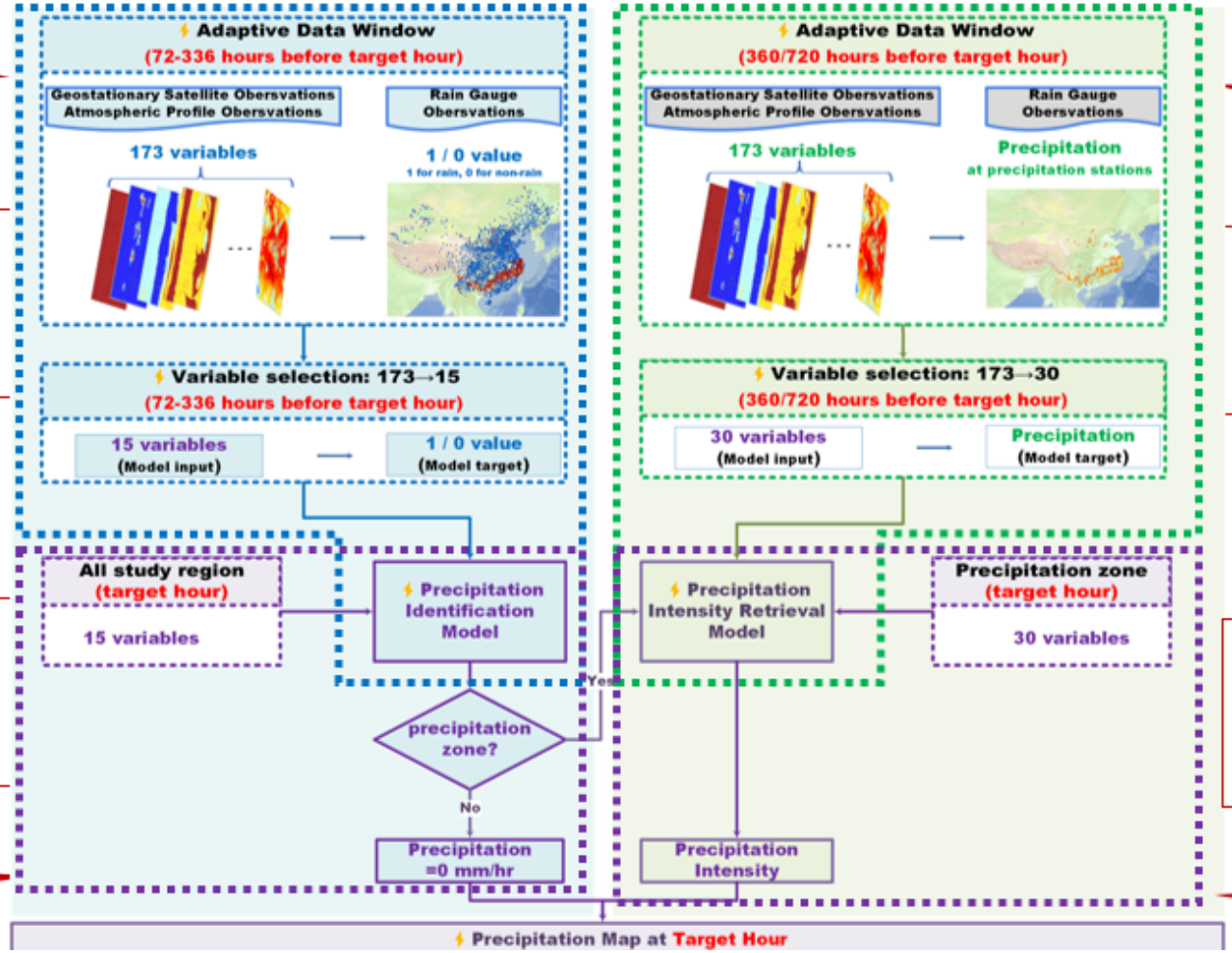
Dynamic Two-step Real-time Precipitation Retrieval Algorithm (D-PRA)

1. Construction of model to identify precipitation areas

2. Construction of precipitation intensity retrieval model

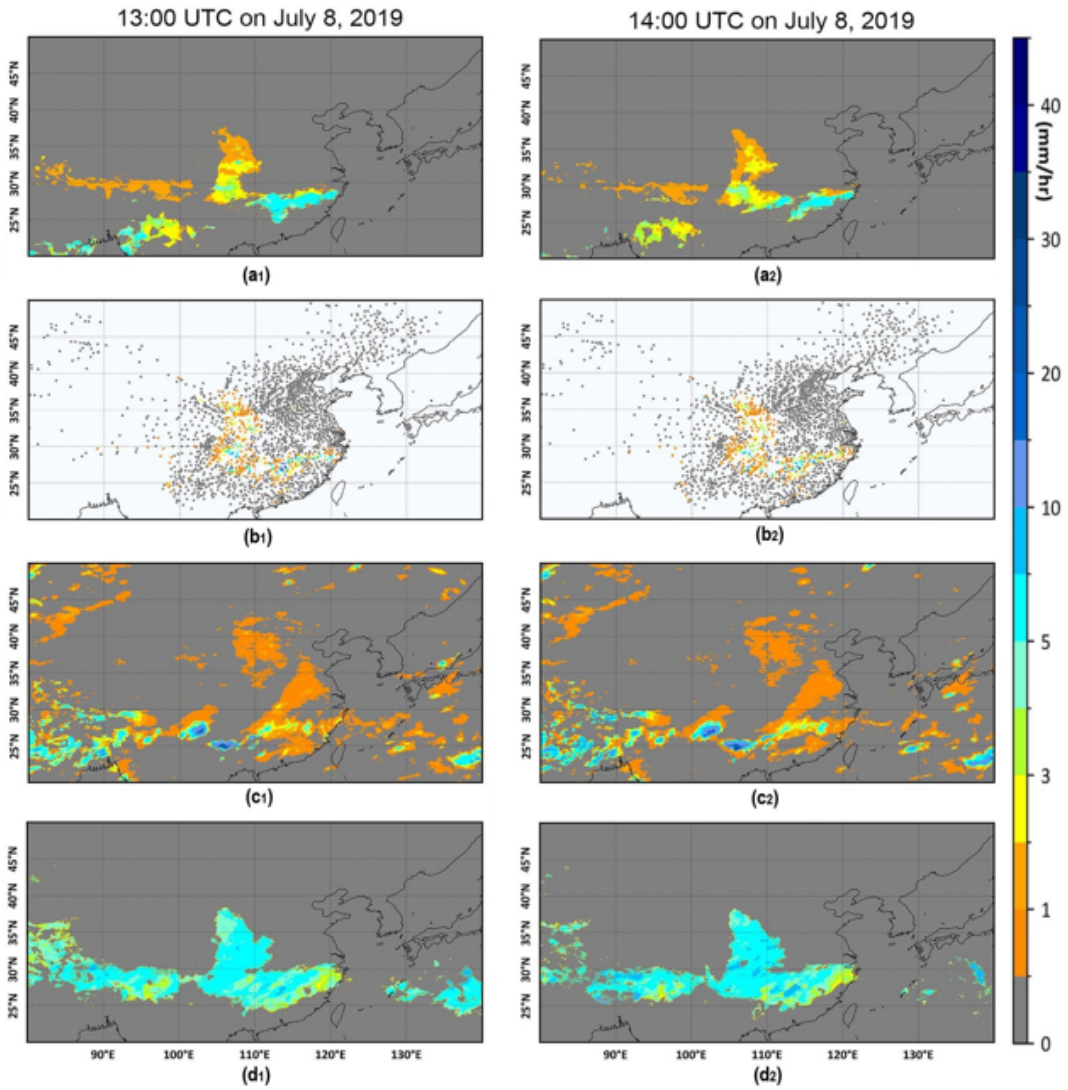
3. Delineate precipitation areas at target hour

4. Retrieve the precipitation rate at target hour



(Cui et al, 2025 IEEE TGRS under review)

Overview of Chinese YSs research



Hourly precipitation at 13:00 UTC (left panel) and 14:00 UTC (right panel) on July 8, 2019:
(a1, a2) D-PRA Estimates;
(b1, b2) Rain Gauge Observations;
(c1, c2) GSMaP_NOW Estimates;
(d1, d2) Fixed-variables Estimates.

(Cui et al, 2025 IEEE TGRS under review)

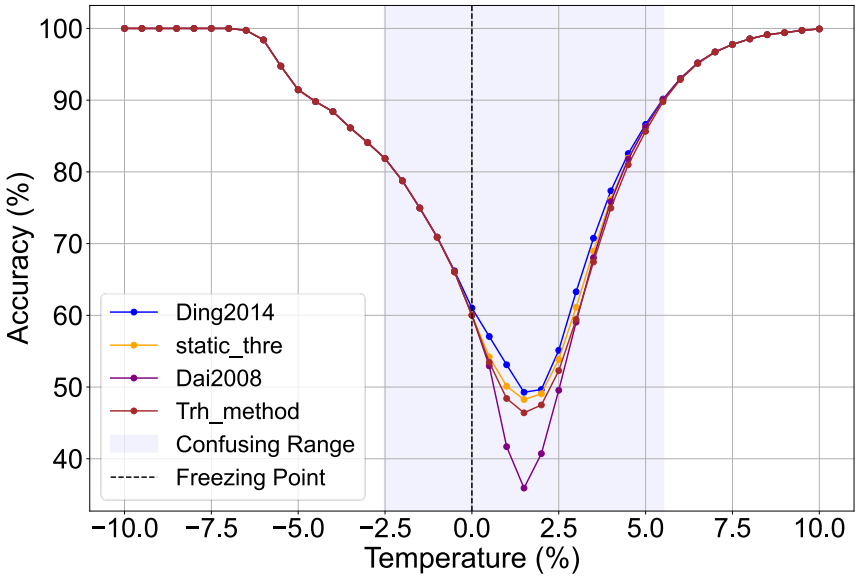
Machine Learning-Based Methods for Precipitation Phase Discrimination in China

Wangkan She

Applying ML in phase discrimination

Accuracy of conventional PPD methods

Dataset: CMA stations observation



Drops below 90% between –7°C and 10°C, even for best-prefroming Ding2014.

static_thre: fixed threshold = 0.6°C. **Ding2014**: Ding et al., 2014. **Dai2008**: Dai, 2008.**Trh_method**: Harder & Pomeroy, 2013.

Input: *longitude, latitude, altitude (geo) wind, Ta, Relative humidty, pressure, precipitation amount(meteo); Tw, Td(calculated)*

?

rain ***sleet*** ***snow***

Optimal INPUT parameter combinations used by each ML method

Method	Optimal input parameter combinations
SVM	*lon, lat, p_s, RH, wind, amount, T_w, T_d*
RF	*lon, lat, p_s, RH, amount, T_w, T_d*
CatBoost	*lon, lat, p_s, RH, amount, T_w, T_d*
CNN	*lon, lat, T_a, p_s, wind, RH, amount, T_w*
MLP	*lon, lat, T_a, p_s, wind, RH, amount, T_w*

Phase recognition ACCURACY of ML and Ding2014 for test set

Method	Overall	A accuracy	B accuracy	C accuracy	D accuracy
Ding2014	83.7%	78.6%	86.0%	84.7%	83.8%
SVM	85.4%	81.8%	87.2%	85.9%	85.3%
RF	86.0%	84.2%	87.3%	85.9%	85.3%
CatBoost	86.7%	87.0%	87.6%	85.7%	85.4%
CNN	87.6%	91.1%	87.3%	85.8%	**85.4%**
MLP	**88.1%**	**91.4%**	**88.3%**	**86.3%**	85.3%

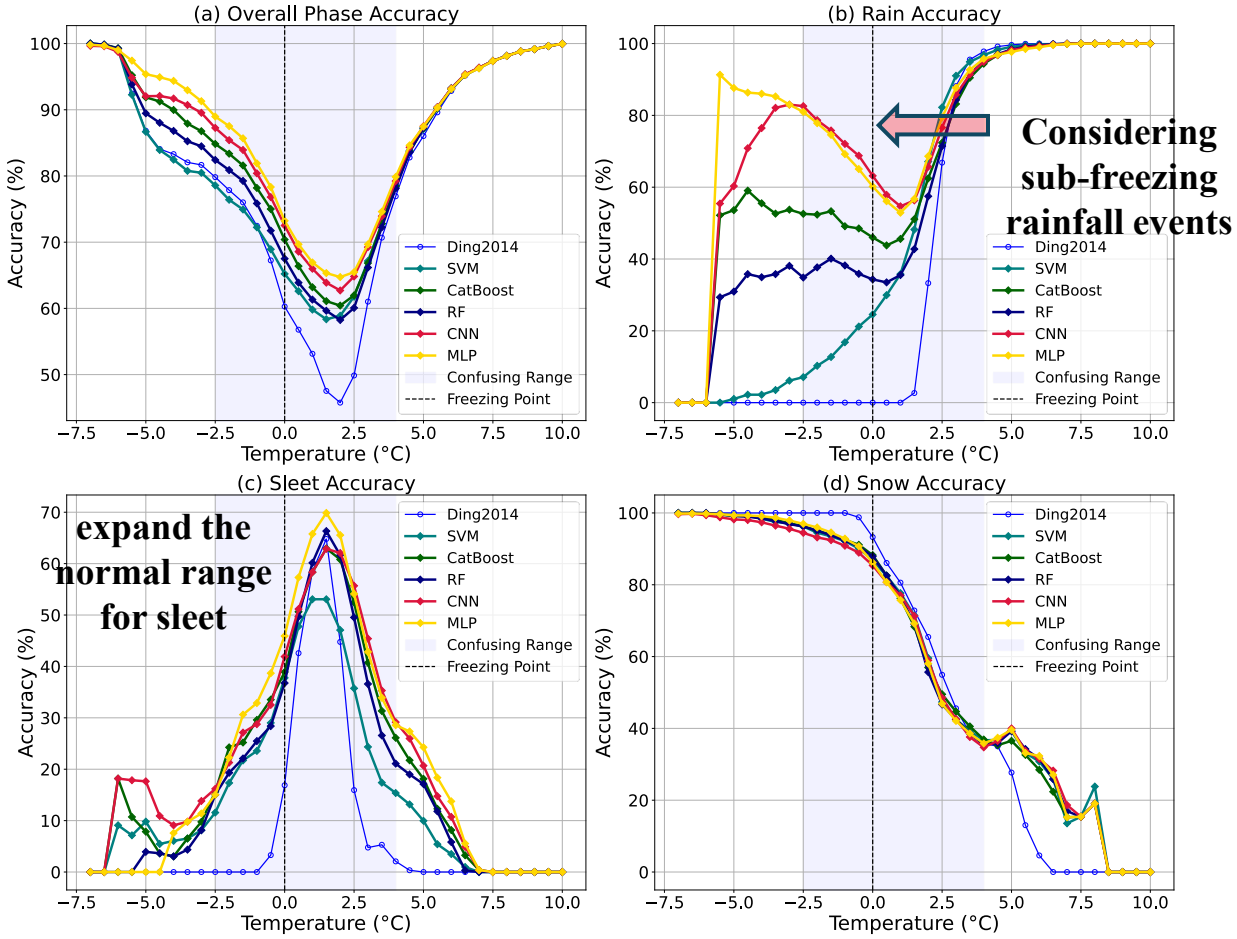
A: Tibetan Plateau; B: South; C:Northwest; D: Northeast & North

SVM (Support Vector Machines) ; **MLP** (Multilayer Perceptron) ; **RF** (Random Forest) ; **CatBoost** (gradient boosting algorithm) ; **CNN** (Convolutional Neural Network)

- **MLP achieved an overall test set accuracy of *88.1%*, improving by *4.4% over Ding2014*.**
- **In *Tibetan Plateau*, the accuracy reached *91.4%*, an *increasement of 12.8% compared to Ding2014.***

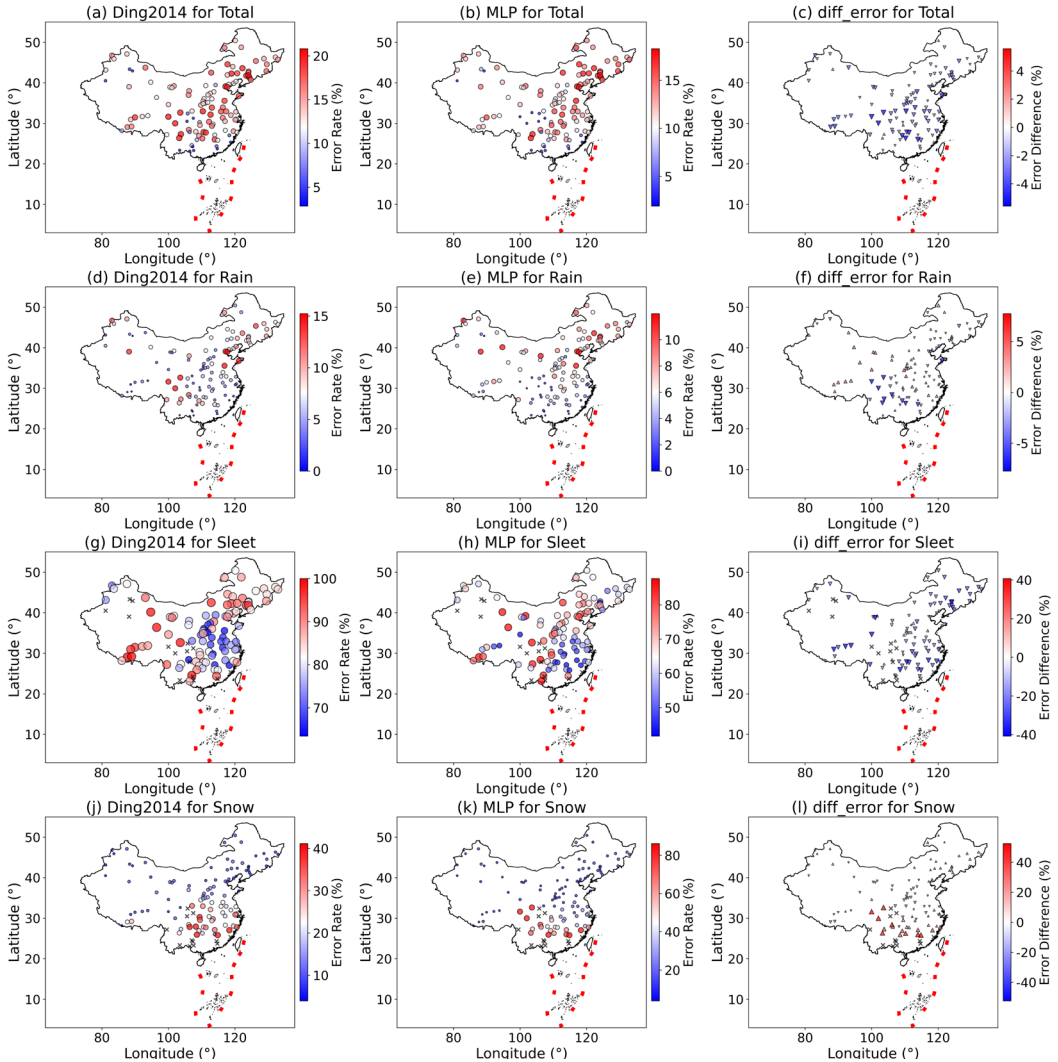
Comparision of MLP & Ding2014

Classification Accuracy by Temperature range



- **MLP *performed well in rainfall (especially frezzing rain)* and showed *high sensitivity to sleet* despite limited sample size.**

Station error map of MLP and Ding2014, and their diff



- ***North-South Contrast*; Improvemnt: *eastern Tibetan Plateau* & *southern China*, where *rainfall and sleet occur frequently*.**


Thank you!